ARTICLE

doi:10.1038/nature10822

Ubiquitin-dependent regulation of COPII coat size and function

Lingyan Jin[1]*, Kanika Bajaj Pahuja[1,2]*, Katherine E. Wickliffe[1], Amita Gorur[1,2], Christine Baumgärtel[1], Randy Schekman[1,2] & Michael Rape[1]

Packaging of proteins from the endoplasmic reticulum into COPII vesicles is essential for secretion. In cells, most COPII vesicles are approximately 60–80 nm in diameter, yet some must increase their size to accommodate 300–400 nm procollagen fibres or chylomicrons. Impaired COPII function results in collagen deposition defects, cranio-lenticulo-sutural dysplasia, or chylomicron retention disease, but mechanisms to enlarge COPII coats have remained elusive. Here, we identified the ubiquitin ligase CUL3–KLHL12 as a regulator of COPII coat formation. CUL3–KLHL12 catalyses the monoubiquitylation of the COPII-component SEC31 and drives the assembly of large COPII coats. As a result, ubiquitylation by CUL3–KLHL12 is essential for collagen export, yet less important for the transport of small cargo. We conclude that monoubiquitylation controls the size and function of a vesicle coat.

The extracellular matrix provides a scaffold for cell attachment and binding sites for membrane receptors, such as integrins, making it essential for the development of all metazoans[1,2]. When engaged with the extracellular matrix, integrins trigger signalling cascades that regulate cell morphology and division, yet in the absence of a functional extracellular matrix, integrins are removed from the plasma membrane by endocytosis[3]. The proper interplay between integrins and the extracellular matrix is particularly important during early development[4], as stem cells depend on integrin-dependent signalling for division and survival[5].

The establishment of the extracellular matrix requires secretion of several proteins, including its major constituent collagen. Following its synthesis in the endoplasmic reticulum, the export of collagen from cells depends on COPII vesicles[6–9], and mutations in genes encoding COPII proteins lead to collagen deposition defects, skeletal aberrations and developmental diseases, such as cranio-lenticulo-sutural dysplasia[10,11].

COPII vesicles are surrounded by a coat consisting of the SAR1 GTPase, SEC23–SEC24 adaptors, and an outer layer of SEC13–SEC31 heterotetramers[12]. These coat proteins self-assemble into cuboctahedral structures with a diameter of approximately 60–80 nm, which are too small to accommodate a procollagen fibre with a length of 300–400 nm[13–15]. Thus, collagen transport in cells must involve factors that are absent from *in vitro* self-assembly reactions. Indeed, TANGO1 (also known as MIA3) and its partner cTAGE5 interact with collagen and SEC23–SEC24, thereby recruiting collagen to nascent COPII coats[16,17]. The deletion of *Tango1* in mice resulted in collagen deposition defects similar to those caused by loss of COPII[18], and mutations in human TANGO1 are associated with premature myocardial infarction[19]. However, TANGO1 is not known to regulate the size of COPII coats and mechanisms that permit the COPII coat to accommodate a large cargo remain poorly understood.

By analysing mouse embryonic stem (ES) cell division, we have identified CUL3–KLHL12 as a regulator of COPII coat formation. CUL3–KLHL12 monoubiquitylates SEC31 and drives assembly of large COPII coats. As a result, ubiquitylation by CUL3–KLHL12 is essential for collagen export, a step that is required for integrin-dependent mouse ES cell division. We conclude that monoubiquitylation determines the size and function of a vesicle coat.

CUL3 regulates mouse ES cell morphology

To provide insight into stem cell-specific division networks, we depleted ubiquitylation enzymes from mouse ES cells and scored for effects on proliferation and morphology. We found that loss of the ubiquitin ligase CUL3 caused mouse ES cells to form tightly packed cell clusters with prominent actin cables and aberrant adhesions, as seen by confocal microscopy analysis of actin and vinculin localization (Fig. 1a). A similar phenotype was observed upon depletion of UBA3, a component of the NEDD8 pathway that activates CUL3 (Supplementary Fig. 1a). CUL3-depleted mouse ES cells were delayed in proliferation (Supplementary Fig. 1b, d), yet retained their pluripotency, as seen by OCT4- and alkaline phosphatase-staining and the absence of differentiation markers in expression analyses (Supplementary Figs 1c, e, f and 2b). In contrast to mouse ES cells, depletion of CUL3 had weaker consequences in fibroblasts (Fig. 1a), although a previously reported increase in multinucleation was observed (Supplementary Fig. 1g; ref. 20).

Several observations show that the mouse ES cell phenotypes were caused by specific depletion of CUL3. First, several short interfering RNAs targeting distinct regions of the *Cul3* messenger RNA had the same effects on mouse ES cells, with a close correlation between knockdown efficiency and strength of phenotype (Supplementary Fig. 2a). Second, microarray analysis showed a strong reduction in *Cul3* mRNA upon siRNA treatment, whereas no other gene was significantly and reproducibly affected (Supplementary Fig. 2b). Third, siRNAs that target closely related proteins, such as other cullins, did not disturb the morphology of mouse ES cells (Supplementary Fig. 2c).

The aberrant morphology of CUL3-depleted mouse ES cells was reminiscent of increased RhoA GTPase activity, which triggers actin filament bundling[21]. Accordingly, a reduction in RhoA levels or inhibition of the RhoA effector kinase ROCK1 rescued CUL3-depleted mouse ES cells from compaction (Supplementary Fig. 3a). Among several possibilities, higher RhoA activity in the absence of CUL3 could result from RhoA stabilization or defective integrin signalling. Stabilization

[1]Department of Molecular and Cell Biology, University of California at Berkeley, California 94720, USA. [2]Howard Hughes Medical Institute, University of California at Berkeley, California 94720, USA.
*These authors contributed equally to this work.

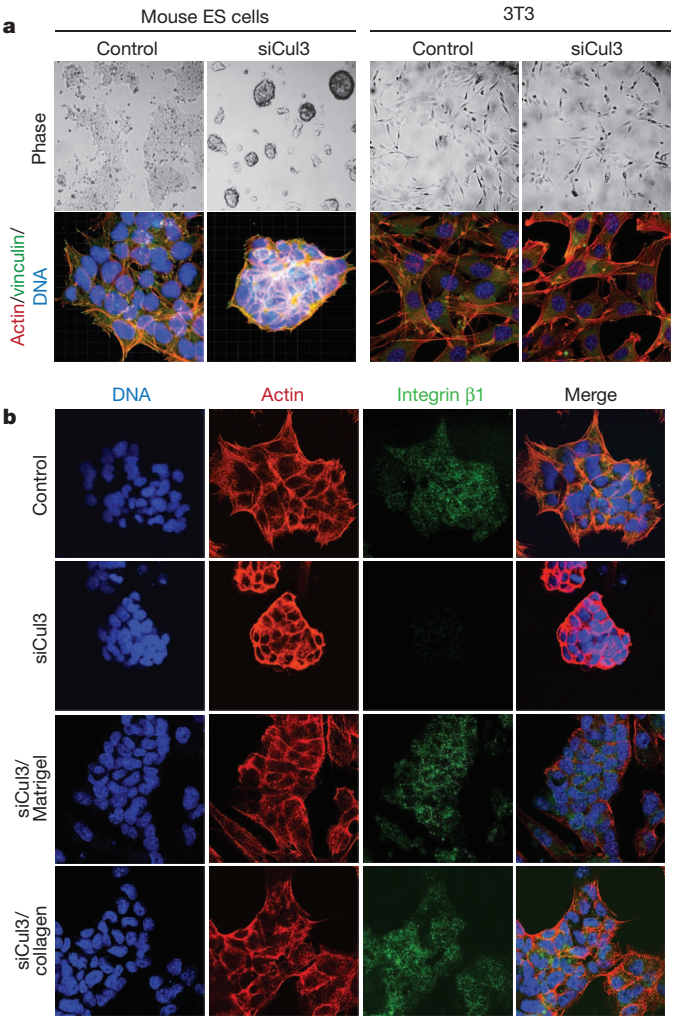

Figure 1 | CUL3 regulates mouse ES cell morphology. **a**, Left, D3 mouse ES cells were plated on gelatin and transfected with siRNAs targeting *Cul3* (siCul3), which resulted in cell clustering (phase microscopy; upper panel) and compaction (confocal microscopy: vinculin, green; actin, red; DNA, blue). Right, Depletion of CUL3 from mouse 3T3 fibroblasts did not cause cell compaction. Phase images original magnification was ×10, fluorescence images ×40. **b**, CUL3 is required for integrin localization to the mouse ES cell plasma membrane. D3 mouse ES cells were plated on gelatin (top two rows), growth-factor-depleted Matrigel or collagen IV. Following CUL3 depletion, cell compaction and integrin-targeting to the plasma membrane were analysed by confocal microscopy (actin, red; integrin β1, green; DNA, blue). Original magnification ×40.

of RhoA by co-depletion of all RhoA-specific CUL3 adaptors, the BACURDs[22], did not affect mouse ES cell morphology (data not shown). By contrast, depletion of components of integrin signalling pathways phenocopied the loss of CUL3 in mouse ES cells (Supplementary Fig. 3b); partial reduction in CUL3 levels showed synthetic lethality with dasatinib, an inhibitor of the SRC kinase that acts downstream of integrin activation (Supplementary Fig. 3c); and integrin β1 was absent from the plasma membrane of CUL3-depleted mouse ES cells (Fig. 1b).

CUL3 could regulate integrin synthesis and trafficking, or it could allow for efficient deposition of extracellular matrix proteins to prevent integrin internalization[3]. To distinguish between these possibilities, we grew mouse ES cells on growth-factor-depleted Matrigel to provide an exogenous extracellular matrix. Strikingly, under these conditions, integrin β1 was found at the plasma membrane of CUL3-depleted mouse ES cells and no cell clustering was observed (Fig. 1b). Thus, CUL3 controls integrin signalling in mouse ES cells, most likely by supporting the establishment of a functional extracellular matrix.

KLHL12 is a key CUL3 adaptor in mouse ES cells

CUL3 recruits substrates through adaptors with BTB domains[23–26], yet siRNA approaches did not yield roles for BTB proteins in ES cells. As an alternative strategy to isolate CUL3 adaptors, we made use of the observation that stem cell regulators are highly expressed in ES cells, but downregulated upon differentiation[27]. Using affinity purification and mass spectrometry, we identified 31 BTB proteins that interact with CUL3 in mouse ES cells (Supplementary Fig. 4a; Supplementary Table 1). When analysed by quantitative polymerase chain reaction with reverse transcription (qRT–PCR) and immunoblot, we found that three adaptors, KLHL12, KBTBD8 and IBTK, were highly expressed in mouse ES cells, but downregulated upon differentiation (Fig. 2a, b and Supplementary Fig. 3d). Next, we depleted these adaptors from mouse ES cells that were sensitized for changes in integrin signalling by treatment with dasatinib. Importantly, depletion of KLHL12, but no other BTB protein, resulted in mouse ES cell compaction, as seen with loss of CUL3 (Fig. 2c). Accordingly, endogenous KLHL12 effectively binds CUL3 in mouse ES cells (Supplementary Fig. 4b). These experiments, therefore, identify KLHL12 as a key substrate-adaptor for CUL3 in mouse ES cells and the CUL3–KLHL12 ubiquitin ligase as an important regulator of mouse ES cell morphology.

CUL3 monoubiquitylates SEC31

To isolate the substrates of CUL3–KLHL12, we constructed 293T cell lines that allowed for the inducible expression of Flag–KLHL12. By affinity chromatography and mass spectrometry, we identified the

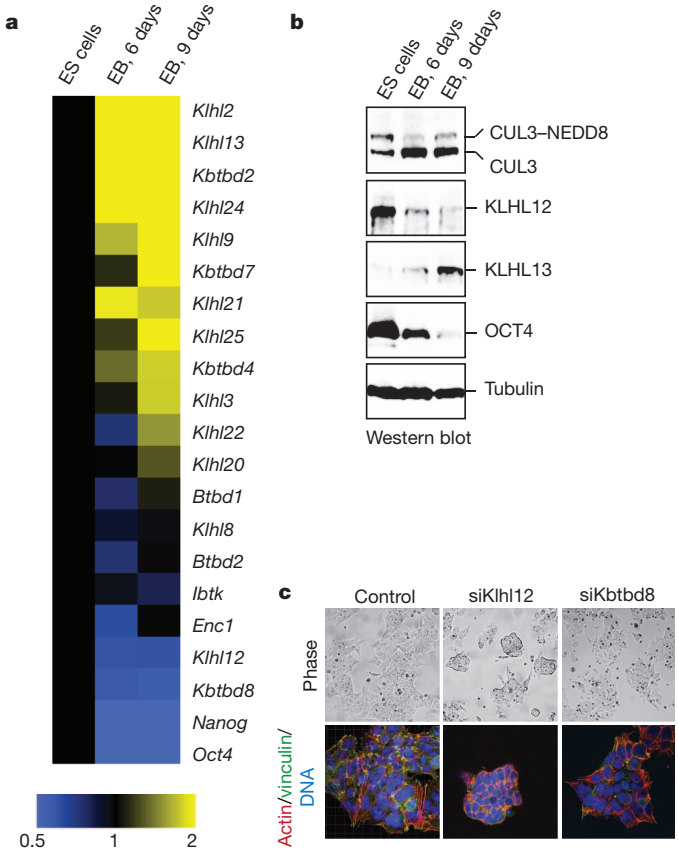

Figure 2 | KLHL12 is a substrate adaptor for CUL3 in mouse ES cells. **a**, D3 mouse ES cells were subjected to differentiation, and mRNA levels of indicated proteins were measured by qRT–PCR. EB, embryoid bodies. **b**, KLHL12 protein is downregulated upon differentiation, as observed by immunoblot of above samples. **c**, KLHL12 is a critical CUL3-adaptor in mouse ES cells. D3 mouse ES cells were sensitized towards altered integrin-signalling with dasatinib and monitored for compaction by phase (upper panel) or confocal microscopy (actin, red; vinculin, green; DNA, blue). Original magnification ×40.

COPII proteins SEC13 and SEC31 as specific binding partners of KLHL12 (Fig. 3a and Supplementary Table 2). Immunoblotting confirmed retention of endogenous SEC13 and SEC31 in KLHL12 purifications, but not in precipitates of other BTB proteins (Supplementary Fig. 5a). As seen in pull-down assays, KLHL12 directly bound SEC31, but not SEC13 (Supplementary Fig. 5c, d), and this interaction was mediated by the amino terminus of SEC31 (Supplementary Fig. 6a) and the Kelch domain of KLHL12 (Supplementary Fig. 6b). In cells, approximately 30% of endogenous KLHL12 was associated with SEC13–SEC31 (Fig. 3b and Supplementary Fig. 5b). Consistent with such a prominent interaction, SEC13–SEC31 and KLHL12 colocalized in punctae, which are likely to represent endoplasmic reticulum exit sites of COPII vesicles (Fig. 3c;[28]). Importantly, siRNAs that compromise COPII resulted in mouse ES cell compaction (Fig. 3d), indicating that CUL3–KLHL12 and the COPII coat act in the same pathway.

In vitro, CUL3–KLHL12 catalysed the monoubiquitylation of SEC31 (Fig. 3e), which was not observed if a KLHL12 mutant with a defective SEC31-binding interface was used (Fig. 3f). SEC31 was also monoubiquitylated in cells, which was strongly increased upon expression of KLHL12 (Fig. 3g). KLHL12 mutants unable to bind SEC31 abolished its monoubiquitylation (Fig. 3h), which is likely to be due to dimerization with and inactivation of endogenous KLHL12 (Fig. 3a and Supplementary Fig. 6c). SEC31 monoubiquitylation was also strongly diminished upon expression of dominant-negative CUL3 (Fig. 3g) or depletion of CUL3–KLHL12 by siRNA (Fig. 3i). As seen upon expression of lysine-free ubiquitin, SEC31 was monoubiquitylated at one preferred and an alternative, less prominently used lysine (Fig. 3g), consistent with proteomic analyses that identified Lys 647 and Lys 1217 in SEC31A as ubiquitylation sites[29,30]. However, neither mutation of these residues nor any other of the 65 lysine residues of SEC31 blocked ubiquitylation by CUL3–KLHL12 (data not shown), revealing flexibility in the actual modification site.

Co-expression of KLHL12 and CUL3 triggered SEC31 multiubiquitylation and degradation (Figs 3g, 4e and Supplementary Fig. 6d), which was not observed with lysine-free ubiquitin (Fig. 3g). However, whereas SEC31 was monoubiquitylated by endogenous CUL3–KLHL12, its multiubiquitylation was only seen when CUL3 and KLHL12 were overexpressed. Depletion of CUL3–KLHL12 or proteasome inhibition did not change SEC31 levels in untransfected cells (Fig. 3i and Supplementary Fig. 6e), and blockade of ubiquitin chain formation or proteasome inhibition did not impair CUL3–KLHL12 function (see Fig. 5). Thus, multiubiquitylation of SEC31 is unlikely a key outcome of CUL3–KLHL12 activity in mouse ES cells. Instead, it seems that CUL3–KLHL12 acts by catalysing monoubiquitylation, with the COPII protein SEC31 as a major substrate.

CUL3 regulates the size of COPII coats

To identify a role for monoubiquitylation by CUL3–KLHL12, we induced KLHL12 expression in cells and followed the fate of SEC31 by microscopy. Shortly after KLHL12 induction, the majority of KLHL12 and SEC31 colocalized in small punctae (Fig. 4a). Over time, these punctae grew into much larger structures that contained most of SEC31, as well as other COPII components, such as SEC13 or SEC24C (Fig. 4a, b). As seen by high-resolution confocal imaging, the large structures were hollow and spherical with a diameter of 200–500 nm, and they were decorated with the proteins of the COPII coat and with KLHL12 (Fig. 4c). Accordingly, thin-section electron microscopy revealed large, crescent-shaped tubules, possibly of endoplasmic reticulum origin, in cells transfected with KLHL12 (Fig. 4d). Immunogold-labelling electron microscopy showed comparable structures of

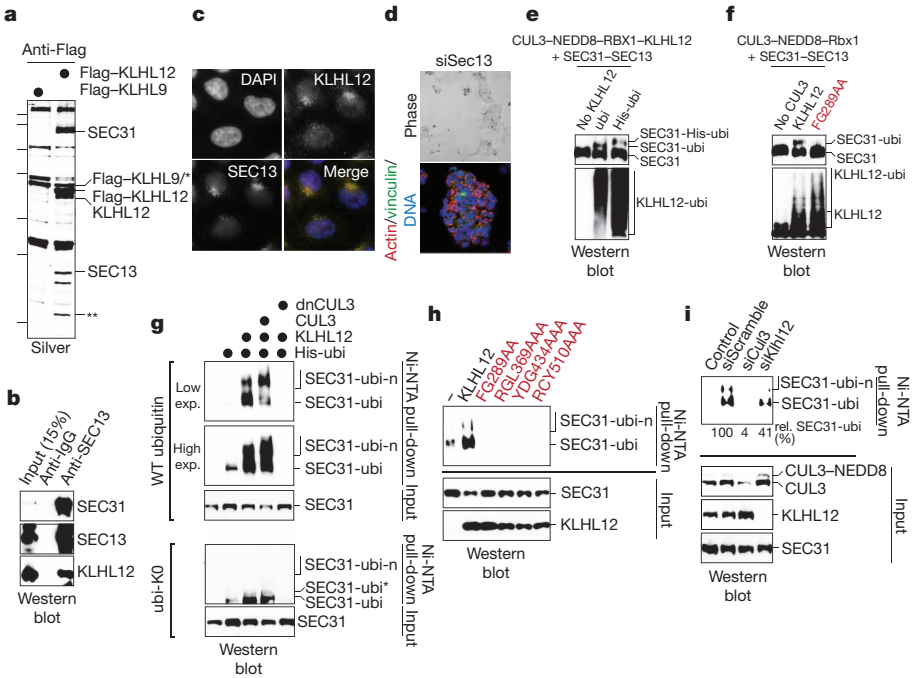

Figure 3 | CUL3–KLHL12 monoubiquitylates SEC31.
a, Immunoprecipitates of Flag–KLHL12 or Flag–Klhl9 were analysed by silver staining and mass spectrometry. Asterisk, non-specific band; double asterisk, breakdown product of KLHL12. **b**, SEC13 was immunoprecipitated from HeLa cell lysates, and SEC31 and KLHL12 were detected by immunoblot. **c**, KLHL12 colocalizes with COPII, as seen by confocal microscopy (KLHL12, green; SEC13, red; DNA, blue). Original magnification ×60. **d**, D3 mouse ES cells grown on gelatin and depleted of SEC13 were analysed for compaction by phase (top) or confocal microscopy (actin, red; vinculin, green; DNA, blue). Original magnification ×40. **e**, CUL3–KLHL12 monoubiquitylates SEC31. CUL3–NEDD8–RBX1 was incubated with KLHL12, SEC13/31 and ubiquitin (ubi) or His-ubiquitin (His-ubi). **f**, *In vitro* ubiquitylation of SEC31 by CUL3–KLHL12 or CUL3–KLHL12(FG289AA) (FG289AA) was performed as above. **g**, SEC31 is monoubiquitylated *in vivo*. Upper panels, ubiquitin conjugates were purified under denaturing conditions from MG132-treated 293T cells expressing His–ubiquitin, haemagglutinin–SEC31, KLHL12, CUL3 or dominant-negative CUL3 (dnCUL3), and analysed by anti-SEC31 Western blot. Lower panels, the same experiment was performed with lysine-free His–ubiquitin, which only allowed SEC31-monoubiquitylation on at least two sites (SEC31-ubi and SEC31-ubi*). SEC31-ubi-n denotes multiubiquitylated SEC31. **h**, Ubiquitin conjugates were purified from 293T cells expressing KLHL12 or SEC31-binding deficient KLHL12 mutants. **i**, CUL3 is essential for SEC31 ubiquitylation *in vivo*. 293T cells were transfected with His–ubiquitin and siRNAs, and ubiquitin conjugates were analysed for SEC31 by Western blot.

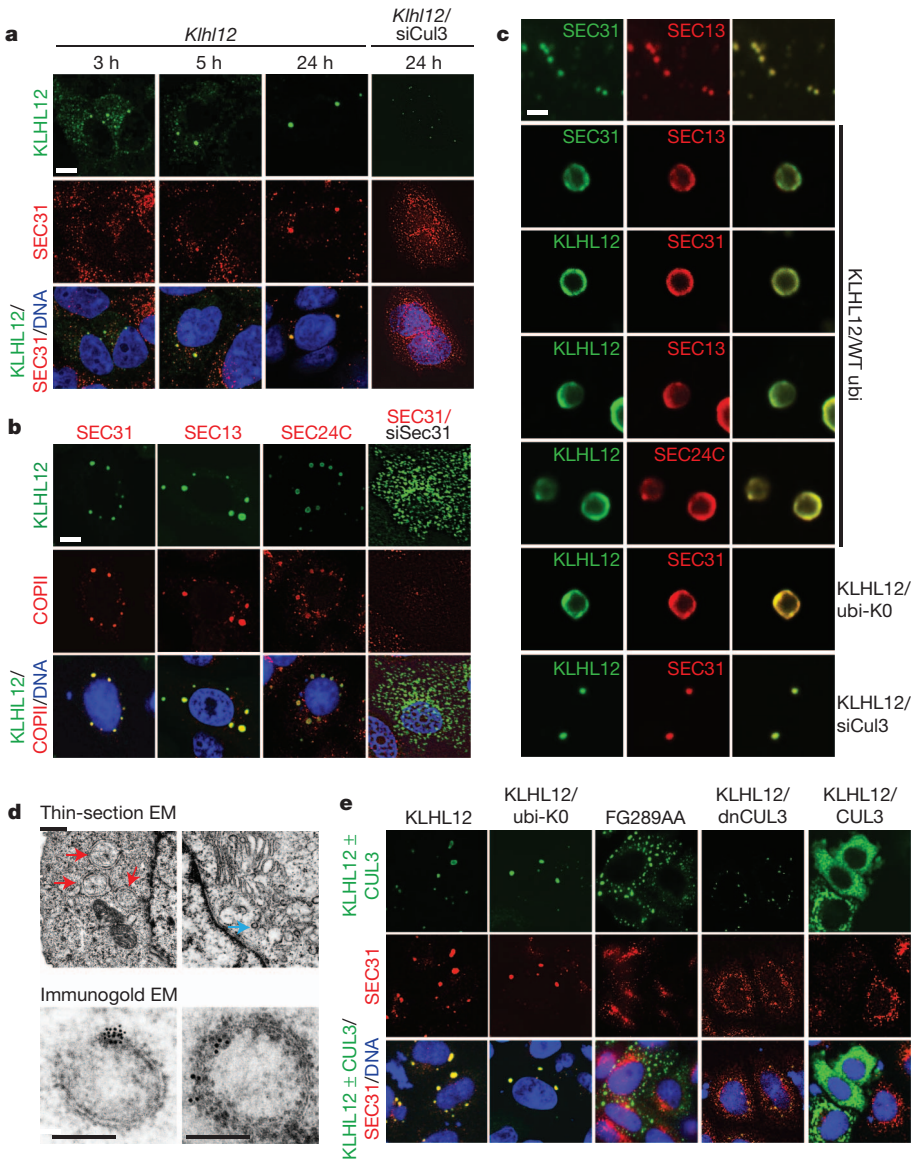

Figure 4 | CUL3–KLHL12-dependent monoubiquitylation enlarges COPII-structures. **a**, Localization of doxycycline (dox)-induced Flag–KLHL12 (dox::*Klhl12*, green) and SEC31 (red) in 293T cells, monitored by confocal microscopy. Scale bar, 3 μm. **b**, KLHL12-expressing HeLa cells were analysed for KLHL12 (green) and SEC31, SEC13 or SEC24C (red) by confocal microscopy. Scale bar, 3 μm. **c**, COPII-structures in HeLa cells transfected with Flag–KLHL12, lysine-free ubiquitin (ubi-K0) or *Cul3*-siRNA, analysed by confocal microscopy. Scale bar, 500 nm. **d**, Upper panel, thin-section electron microscopy (EM) of KLHL12-expressing or control HeLa cells (red arrow, KLHL12-dependent structures; blue arrow, small control vesicles). Scale bar, 500 nm. Lower panel, immunogold-EM of KLHL12 in transiently transfected HeLa (left) or stable 293T cells (right). Scale bar, 200 nm. **e**, HeLa cells transfected with Flag–KLHL12, lysine-free ubiquitin, Flag–KLHL12(FG289AA), Flag–CUL3(1–250) or Flag–CUL3 were analysed for localization of KLHL12/CUL3 (green) and SEC31 (red) by confocal microscopy. Original magnification ×40.

200–500 nm that were decorated with KLHL12 (Fig. 4d). The KLHL12-dependent structures neither contained a *cis*-Golgi protein; ERGIC-53, which is absent from procollagen transport vesicles[31]; endoplasmic reticulum membrane markers that do not accumulate at endoplasmic reticulum exit sites[32]; nor endosomal or autophagosomal markers (Supplementary Fig. 7a–c). Importantly, SEC31-binding deficient mutants, including KLHL12(FG289AA), neither colocalized with SEC31 nor induced formation of large structures (Fig. 4e and Supplementary Fig. 7d), and depletion of SEC31 blocked formation of large structures by KLHL12 (Fig. 4b). Thus, binding of KLHL12 to SEC31 triggers formation of large COPII-containing structures.

When KLHL12 was expressed with a CUL3 mutant that blocks SEC31 ubiquitylation (CUL3(1–250)), COPII structures were not enlarged (Fig. 4e). In addition, depletion of CUL3 by siRNAs, which also abolishes SEC31 monoubiquitylation, prevented formation of large COPII structures by KLHL12 (Fig. 4a, c). By contrast, if KLHL12 was expressed with lysine-free ubiquitin to allow mono-, but not multiubiquitylation, large COPII structures were readily detected (Fig. 4c, e), and these structures were enriched for ubiquitin, consistent with monoubiquitylation being non-proteolytic (Supplementary Fig. 7e). Thus, monoubiquitylation by CUL3–KLHL12 promotes formation of large COPII structures, which probably represent a mixture of nascent coats at endoplasmic reticulum exit sites and budded coats on large COPII vesicles or tubules.

CUL3 is required for collagen export

Our screen linked CUL3–KLHL12 to the establishment of the stem cell extracellular matrix, which requires collagen secretion. Thus, the CUL3–KLHL12-dependent increase in COPII size might function to promote collagen export from the endoplasmic reticulum. To test this hypothesis, we expressed KLHL12 in IMR90 cells, which at steady state accumulate collagen in the endoplasmic reticulum due to inefficient export. Strikingly, KLHL12, but not KLHL12(FG289AA) or unrelated BTB proteins, triggered depletion of procollagen I from intracellular endoplasmic reticulum pools (Fig. 5a). As a result, increased collagen levels were detected in the supernatant of cells expressing KLHL12, but not KLHL12(FG289AA) (Fig. 5b). When secretion was inhibited with brefeldin A, or if collagen folding in the endoplasmic reticulum was impaired by removal of ascorbate from the medium, procollagen remained within KLHL12-expressing cells (Fig. 5a). Time-resolved experiments showed that KLHL12 strongly accelerated collagen export from IMR90 cells (Fig. 5c). Shortly after inducing secretion, KLHL12 and collagen were detected at overlapping locations (Supplementary Fig. 7f), all of which indicates that CUL3–KLHL12 facilitates collagen traffic from the endoplasmic reticulum.

Blockade of SEC31 ubiquitylation by dominant-negative CUL3 interfered with the KLHL12-dependent export of collagen from IMR90 cells (Supplementary Fig. 8a). Similarly, depletion of CUL3–KLHL12 from engineered HT1080 fibrosarcoma cells severely

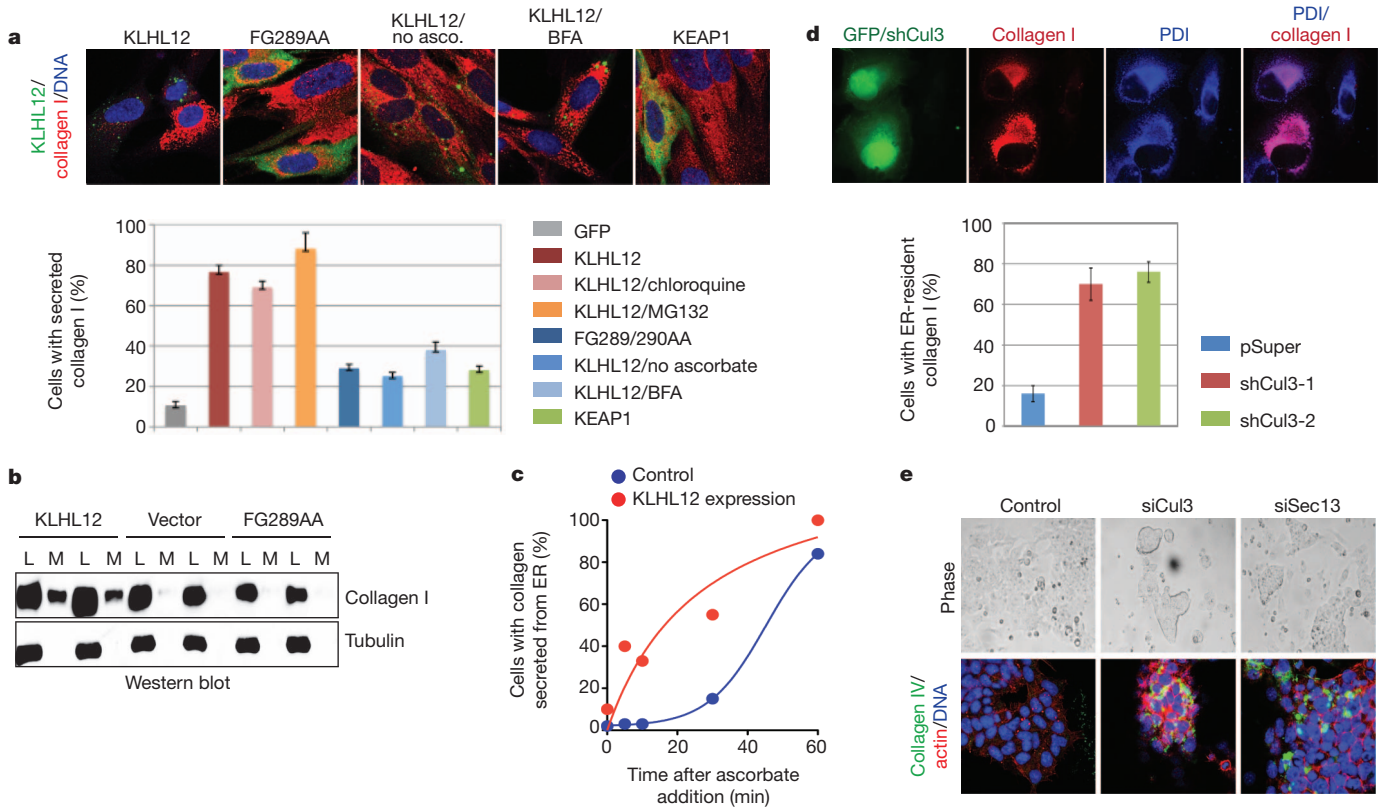

Figure 5 | CUL3–KLHL12 promotes collagen export. **a**, IMR90 cells transfected with Flag–KLHL12, Flag–KLHL12(FG289AA) or Flag–KEAP1 were analysed by confocal microscopy (BTB, green; collagen-I, red; DNA, blue). When noted, cells were treated with chloroquine, MG132, brefeldin A (BFA) or dialysed medium lacking ascorbate. Errors bars, standard deviation $n = 3$. Original magnification ×60. **b**, Cell lysate (L) or culture medium (M) of IMR90 cells transfected with Flag–KLHL12 or Flag–KLHL12(FG289AA) was analysed by immunoblotting. **c**, Collagen I localization was analysed in IMR90 cells expressing KLHL12, after re-addition of ascorbate. Original magnification ×40. **d**, HT1080 cells stably expressing collagen I were transfected with shRNAs against *Cul3* and analysed by confocal microscopy (transfection control green fluorescent protein (GFP), green; protein disulphide isomerase (PDI), blue; collagen I, red). Error bars, standard deviation $n = 3$. Original magnification ×60. **e**, D3 mouse ES cells were treated with control siRNAs or siRNAs targeting *Cul3* or *Sec13* and analysed by confocal microscopy (collagen IV, green; actin, red; DNA, blue). Original magnification ×40.

impaired collagen export, and most cells retained high levels of collagen in their endoplasmic reticulum (Fig. 5d and Supplementary Fig. 8b). In contrast, smaller COPII cargoes, such as fibronectin or EGF receptor, were properly localized in the absence of CUL3 (Supplementary Fig. 8c, d). Similar observations were made in mouse ES cells, where depletion of CUL3 led to a strong intracellular accumulation of collagen IV, comparable to the effects observed upon loss of SEC13 (Fig. 5e and Supplementary Fig. 8e). Thus, CUL3–KLHL12 is required for collagen export, whereas it is less important for the trafficking of smaller COPII cargo.

If promoting collagen export were the key role of CUL3 in mouse ES cells, the phenotypes of CUL3 depletion might be mitigated by addition of collagen *in trans*. Indeed, this was the case: when mouse ES cells were plated on purified collagen IV, depletion of CUL3 did not cause cell clustering, and integrin β1 was detected at the plasma membrane (Fig. 1b). We conclude that promoting collagen secretion is a key a function of CUL3, in agreement with its role in driving the assembly of large COPII coats.

Discussion

In this study, we have identified CUL3–KLHL12 as an essential regulator of collagen export, which is required for mouse ES cell division. Deletion of *Cul3* in mice results in early embryonic lethality with completely disorganized extraembryonic tissues[33], a phenotype that can in part be attributed to its role in collagen secretion. Moreover, KLHL12 has been identified as an autoantigen in the connective tissue disorder Sjogren's syndrome[34], raising the possibility that aberrant function of CUL3–KLHL12 might be related to disease.

CUL3–KLHL12 monoubiquitylates SEC31 and promotes formation of large COPII coats that can accommodate unusually shaped cargo. As a result, CUL3 is essential for the secretion of procollagen fibres, whereas it is not required for the transport of smaller or more flexible molecules, such as fibronectin, EGF receptor or integrin β1. Thus, CUL3–KLHL12 seems to be specifically required for the COPII-dependent transport of large cargo.

How ubiquitylation affects COPII coat size or structure is not known. None of the 65 lysine residues of SEC31 was essential for ubiquitylation by CUL3–KLHL12, showing that CUL3 can target alternative lysine residues if the primary site is blocked. Despite this flexibility, CUL3–KLHL12 does not stoichiometrically ubiquitylate SEC31. Thus, if SEC31 ubiquitylation performs a structural role, then few ubiquitylated molecules must suffice to produce large COPII coats, and these vesicles must tolerate considerable variation in the modification site. Alternatively, as often seen with monoubiquitylated proteins, modified SEC31 might recruit an effector that delays COPII budding or promotes coat polymerization. As CUL3–KLHL12 ubiquitylates other proteins[35], SEC31 may not be its only substrate in the secretory pathway. Identification of the complete set of CUL3–KLHL12 substrates and potential effector molecules should reveal the mechanism underlying the ubiquitin-dependent regulation of vesicle size.

Our findings have the potential to be translated into therapeutic strategies. We envision that agonists of CUL3–KLHL12 function mitigate consequences of *Sec23A* mutations in cranio-lenticulo-sutural dysplasia or *Sar1* mutations in chylomicron retention disease[10,11]. By contrast, interfering with CUL3 activity may counteract increased collagen

deposition during fibrosis or keloid formation[36]. Given the strong clustering phenotypes observed in CUL3-depleted mouse ES cells, inhibition of CUL3–KLHL12 might impair the proliferation of metastatic cells, which display features of undifferentiated cells[37,38]. Thus, our identification of CUL3–KLHL12 as a regulator of COPII size and function provides an exciting starting point to understand and therapeutically exploit key events in protein trafficking.

METHODS SUMMARY

For stem cell culture, mouse D3 ES cells were maintained in GIBCO Dulbecco's Modified Eagle ES cell medium containing 15% FBS, 1× sodium pyruvate, 1× non-essential amino acids, 1 mM β-mercaptoethanol and 1,000 U ml^{-1} leukaemia inhibitory factor (Millipore), and grown on gelatin-coated culture plates. Doxycycline-inducible 293T Trex Flag–BTB stable cell lines were made with the Flp-In T-REx 293 Cell Line system (Invitrogen) and maintained with blasticidin and hydromycin B.

For screening, two siRNA oligonucleotides were designed against 40 mouse ubiquitin ligases (Qiagen). siRNA oligonucleotides (10 pmol) and Lipofectamine 2000 were pre-incubated in a gelatin-coated 96-well plate. D3 mouse ES cells were seeded at 15,000 cells per well on top of the siRNA mixture, and the morphology of ES cell colonies was examined by bright-field microscopy 48 h after transfection.

To identify CUL3–KLHL12 substrates, doxycycline-inducible 239T cell lines expressing Flag–KLHL12 or Flag–KLHL9 were induced for 48 h. Cleared lysate was subjected to anti-Flag M2 affinity gel (Sigma), and precipitations were eluted with 3×Flag peptide (Sigma). Concentrated eluates were analysed by SDS–PAGE, and specific bands were identified by mass spectrometry analysis by the Vincent J. Coates Proteomics/Mass Spectrometry Laboratory.

For *in vitro* ubiquitylation reactions, CUL3/RBX1 purified from Sf9 cells was conjugated to NEDD8 using recombinant APPBP1–UBA3, UBC12 (also known as UBE2M) and NEDD8. KLHL12 purified from *Escherichia coli* and SEC31A–SEC13 complexes from Sf9 cells were added together with energy mix, E1, UBCH5C (also known as UBE2D3) and ubiquitin and incubated at 30 °C for 1 h.

For confocal microscopy, cells fixed in paraformaldehyde and permeabilized with Triton X-100 were incubated with primary antibodies for 2 h and Alexa-labelled secondary antibodies (Invitrogen) for 1 h. Pictures were taken on Zeiss LSM 510 and 710 confocal microscopes and analysed with LSM image browser and Imaris 3D imaging processing software. Images were processed for contrast enhancement to remove noise.

Full Methods and any associated references are available in the online version of the paper at www.nature.com/nature.

Received 3 August 2011; accepted 3 January 2012.

1. Leitinger, B. Transmembrane collagen receptors. *Annu. Rev. Cell Dev. Biol.* **27,** 265–290 (2011).
2. Wickström, S. A., Radovanac, K. & Fassler, R. Genetic analyses of integrin signaling. *Cold Spring Harb. Perspect. Biol.*. doi:10.1101/cshperspect.a005116 (30 December 2010).
3. Caswell, P. T., Vadrevu, S. & Norman, J. C. Integrins: masters and slaves of endocytic transport. *Nature Rev. Mol. Cell Biol.* **10,** 843–853 (2009).
4. Stephens, L. E. *et al.* Deletion of beta 1 integrins in mice results in inner cell mass failure and peri-implantation lethality. *Genes Dev.* **9,** 1883–1895 (1995).
5. Chen, S. S., Fitzgerald, W., Zimmerberg, J., Kleinman, H. K. & Margolis, L. Cell-cell and cell-extracellular matrix interactions regulate embryonic stem cell differentiation. *Stem Cells* **25,** 553–561 (2007).
6. Lang, M. R., Lapierre, L. A., Frotscher, M., Goldenring, J. R. & Knapik, E. W. Secretory COPII coat component Sec23a is essential for craniofacial chondrocyte maturation. *Nature Genet.* **38,** 1198–1203 (2006).
7. Townley, A. K. *et al.* Efficient coupling of Sec23–Sec24 to Sec13–Sec31 drives COPII-dependent collagen secretion and is essential for normal craniofacial development. *J. Cell Sci.* **121,** 3025–3034 (2008).
8. Sarmah, S. *et al.* Sec24D-dependent transport of extracellular matrix proteins is required for zebrafish skeletal morphogenesis. *PLoS ONE* **5,** e10367 (2010).
9. Ohisa, S., Inohaya, K., Takano, Y. & Kudo, A. *sec24d* encoding a component of COPII is essential for vertebra formation, revealed by the analysis of the medaka mutant, *vbi*. *Dev. Biol.* **342,** 85–95 (2010).
10. Boyadjiev, S. A. *et al.* Cranio-lenticulo-sutural dysplasia is caused by a *SEC23A* mutation leading to abnormal endoplasmic-reticulum-to-Golgi trafficking. *Nature Genet.* **38,** 1192–1197 (2006).
11. Fromme, J. C. *et al.* The genetic basis of a craniofacial disease provides insight into COPII coat assembly. *Dev. Cell* **13,** 623–634 (2007).
12. Jensen, D. & Schekman, R. COPII-mediated vesicle formation at a glance. *J. Cell Sci.* **124,** 1–4 (2011).
13. Stagg, S. M. *et al.* Structural basis for cargo regulation of COPII coat assembly. *Cell* **134,** 474–484 (2008).
14. Fath, S., Mancias, J. D., Bi, X. & Goldberg, J. Structure and organization of coat proteins in the COPII cage. *Cell* **129,** 1325–1336 (2007).
15. Fromme, J. C. & Schekman, R. COPII-coated vesicles: flexible enough for large cargo? *Curr. Opin. Cell Biol.* **17,** 345–352 (2005).
16. Saito, K. *et al.* TANGO1 facilitates cargo loading at endoplasmic reticulum exit sites. *Cell* **136,** 891–902 (2009).
17. Saito, K. *et al.* cTAGE5 mediates collagen secretion through interaction with TANGO1 at endoplasmic reticulum exit sites. *Mol. Biol. Cell* **22,** 2301–2308 (2011).
18. Wilson, D. G. *et al.* Global defects in collagen secretion in a *Mia3/TANGO1* knockout mouse. *J. Cell Biol.* **193,** 935–951 (2011).
19. Kathiresan, S. *et al.* Genome-wide association of early-onset myocardial infarction with single nucleotide polymorphisms and copy number variants. *Nature Genet.* **41,** 334–341 (2009); corrigendum **41,** 762 (2009).
20. Sumara, I. *et al.* A Cul3-based E3 ligase removes Aurora B from mitotic chromosomes, regulating mitotic progression and completion of cytokinesis in human cells. *Dev. Cell* **12,** 887–900 (2007).
21. Shaw, L. M., Rabinovitz, I., Wang, H. H., Toker, A. & Mercurio, A. M. Activation of phosphoinositide 3-OH kinase by the α6β4 integrin promotes carcinoma invasion. *Cell* **91,** 949–960 (1997).
22. Chen, Y. *et al.* Cullin mediates degradation of RhoA through evolutionarily conserved BTB adaptors to control actin cytoskeleton structure and cell movement. *Mol. Cell* **35,** 841–855 (2009).
23. Furukawa, M. & Xiong, Y. BTB protein Keap1 targets antioxidant transcription factor Nrf2 for ubiquitination by the Cullin 3-Roc1 ligase. *Mol. Cell. Biol.* **25,** 162–171 (2005).
24. Geyer, R., Wee, S., Anderson, S., Yates, J. & Wolf, D. A. BTB/POZ domain proteins are putative substrate adaptors for cullin 3 ubiquitin ligases. *Mol. Cell* **12,** 783–790 (2003).
25. Pintard, L. *et al.* The BTB protein MEL-26 is a substrate-specific adaptor of the CUL-3 ubiquitin-ligase. *Nature* **425,** 311–316 (2003).
26. Xu, L. *et al.* BTB proteins are substrate-specific adaptors in an SCF-like modular ubiquitin ligase containing CUL-3. *Nature* **425,** 316–321 (2003).
27. Young, R. A. Control of the embryonic stem cell state. *Cell* **144,** 940–954 (2011).
28. Hughes, H. *et al.* Organisation of human ER-exit sites: requirements for the localisation of Sec16 to transitional ER. *J. Cell Sci.* **122,** 2924–2934 (2009).
29. Kim, W. *et al.* Systematic and quantitative assessment of the ubiquitin-modified proteome. *Mol. Cell* **44,** 325–340 (2011).
30. Emanuele, M. J. *et al.* Global identification of modular cullin-RING ligase substrates. *Cell* **147,** 459–474 (2011).
31. Stephens, D. J. & Pepperkok, R. Imaging of procollagen transport reveals COPI-dependent cargo sorting during ER-to-Golgi transport in mammalian cells. *J. Cell Sci.* **115,** 1149–1160 (2002).
32. Zhu, W. *et al.* Bcl-2 mutants with restricted subcellular location reveal spatially distinct pathways for apoptosis in different cell types. *EMBO J.* **15,** 4130–4141 (1996).
33. Singer, J. D., Gurian-West, M., Clurman, B. & Roberts, J. M. Cullin-3 targets cyclin E for ubiquitination and controls S phase in mammalian cells. *Genes Dev.* **13,** 2375–2387 (1999).
34. Uchida, K. *et al.* Identification of specific autoantigens in Sjogren's syndrome by SEREX. *Immunology* **116,** 53–63 (2005).
35. Angers, S. *et al.* The KLHL12–Cullin-3 ubiquitin ligase negatively regulates the Wnt–β-catenin pathway by targeting Dishevelled for degradation. *Nature Cell Biol.* **8,** 348–357 (2006).
36. Schäfer, M. & Werner, S. Cancer as an overhealing wound: an old hypothesis revisited. *Nature Rev. Mol. Cell Biol.* **9,** 628–638 (2008).
37. Nguyen, D. X., Bos, P. D. & Massague, J. Metastasis: from dissemination to organ-specific colonization. *Nature Rev. Cancer* **9,** 274–284 (2009).
38. Zhang, X. H. *et al.* Latent bone metastasis in breast cancer tied to Src-dependent survival signals. *Cancer Cell* **16,** 67–78 (2009).

Acknowledgements We thank B. Schulman for advice and gifts of cDNAs and proteins. We are grateful to J. Schaletzky for critically reading the manuscript and many discussions. We thank the members of the Rape and Schekman labs for advice and suggestions, L. Lim for providing *Cul3*-shRNAs, C. Glazier for contributions on BTB protein cloning, and A. Fischer and M. Richner for tissue culture support. This work was funded by grants from the Pew Foundation (M.R.), the NIH (NIGMS-RO1, M.R.; NIH Director's New Innovator Award, M.R.), and the Howard Hughes Medical Institute (R.S.). L.J. was funded by a CIRM predoctoral fellowship; she is a Tang fellow. K.B.P. is an HFSP long term post-doctoral fellow.

Author Contributions Experiments were designed by L.J., K.B.P., R.S. and M.R.; L.J. performed the mouse ES cell screen, identified KLHL12 and SEC31, and analysed the role of CUL3 in COPII formation in cells and in collagen export in mouse ES cells; K.B.P. analysed collagen export in fibroblasts; K.E.W. analysed COPII formation in cells; C.B. identified inactive KLHL12; A.G. performed electron micrscopy; L.J., K.B.P. and M.R. prepared the manuscript.

Author Information Reprints and permissions information is available at www.nature.com/reprints. The authors declare no competing financial interests. Readers are welcome to comment on the online version of this article at www.nature.com/nature. Correspondence and requests for material should be addressed to M.R. (mrape@berkeley.edu).

METHODS

Plasmids, protein, antibodies. Human *Cul3* and *Klhl12* were cloned into pcDNA4 and pcDNA5 vectors for expression in mammalian cells. *Cul3*, *Sec31A* and *Sec13* were also cloned into pCS2 vector for IVT/T and expression in mammalian cells. pcDNA4-Cul3^{N250} contains the first cullin repeat of the N-terminal CUL3 (amino acids 1–250) which is sufficient for binding BTB proteins, but not RBX1 and serves as a dominant negative for CUL3/BTB-mediated ubiquitylation. The KLHL12 mutants FG289AA, RL342AA, RGL369AAA, RE416AA, YDG434AAA and RCY510AAA were made by site-directed mutagenesis.

CUL3 and RBX1 were cloned into pFastBac, co-expressed in Sf9 ES insect cells using the Bac-to-Bac baculovirus expression system (Invitrogen) and purified as a complex by Ni-NTA agarose (Qiagen). Similarly, the SEC31A–SEC13 heterodimer and UBA1 were purified from Sf9 ES insect cells. *UbcH5c* and *Ubc12* were cloned into pQE vector and purified from BL21(DE3) bacterial cells. Ubiquitin was cloned into pET and pCS2 vector with a N-terminal 6×His tag. The pET-His-ubiquitin was used for bacterial purification whereas pCS2-His-ubiquitin was expressed in mammalian cells. Wild-type ubiquitin, APPBP1–UBA3 and NEDD8 were purchased from Boston Biochem.

To purify recombinant KLHL12 for ubiquitylation assays, we expressed pMAL-TEV-KLHL12-his and pMAL-TEV-KLHL12^{FG289AA}-his in BL21(DE3) cells, purified the proteins on amylose resin, cleaved them by TEV protease, and re-purified them on Ni-NTA agarose. Wild-type *Klhl12* and mutants were also cloned into pMAL vector and purified as maltose-binding protein (MBP)-tagged proteins for in-vitro protein binding assays.

All shRNAs were cloned in pSuper-GFP neo vector (from Oligoengine) into BglII and XhoI sites. The GFP–BCL2–CYB5 construct, a fusion between Bcl2 and cytochrome *b*5, was purchased from Clontech.

We raised mouse monoclonal antibodies against human KLHL12 and human KLHL13. Both antibodies are available at Promab Biotechnologies (catalogue nos 30058 and 30067). We also raised antibodies against SEC13, SEC24C and SEC24D. Other antibodies used in this study are: CUL3 (Bethyl Laboratories, catalogue no. A301-109A), SEC31A (BD Biosciences, catalogue no. 612350), collagen IV (Abcam, catalogue no. ab19808), anti-Flag (Sigma, catalogue nos F3165, F7425), Ubiquitin (Santa Cruz, catalogue no. sc-8017, P4D1), rhodamine phalloidin (Invitrogen, catalogue no. R415), PDI (1D3) (Assay Designs, catalogue no. SPA-891), anti LC-3 (Sigma, catalogue no. L-7543), anti-alpha tubulin (DM1A, Abcam, catalogue no. ab7291), anti-fibronectin (Abcam, ab2413), anti-GM130 (BD Biosciences, catalogue no. 610822), and anti-EGFR (Ab12, Neomarkers, MS-400P1). LF-67 (anti-sera for Type I procollagen) was obtained as a gift from L. Fisher.

Cell culture. The D3 mouse embryonic stem cells (mouse ES cell) were maintained in ES cell medium containing 15% FBS, 1× sodium pyruvate, 1× non-essential amino acids, 1 mM β-mercaptoethanol and 1,000 U ml^{-1} leukaemia inhibitory factor (Millipore, catalogue no. ESG1107) in GIBCO Dulbecco's Modified Eagle Medium, and grown on 0.1% gelatin-coated tissue culture plates. HeLa cells, 293T cells, 3T3 cells and IMR90 cells were maintained in DMEM plus 10% FBS. Dialysed FBS was bought from HyClone. The doxycycline-inducible 293T Trex KLHL12-3×Flag stable cell line was made with Flp-In T-REx 293 Cell Line system from Invitrogen. Stable cell lines expressing other BTB-proteins were generated accordingly. These cell lines were maintained with 10% TET(−) FBS, blasticidin and hydromycin B as instructed and expression was induced by 1 μg ml^{-1} doxycycline.

Human lung fibroblasts IMR-90 cells were obtained from the Corielle Institute: NIA (National Institute on Ageing) Ageing Cell Repository. For generating procollagen stable HT-1080cell lines, we cloned proalpha(1) into a pRMc/CMV-vector and selected for neomycin resistance[39]. This vector was provided as a gift by N. Bulleid. Cells were kept in a 37 °C incubator with 5% CO_2.

siRNA screen in mouse ES cells. siRNA oligonucleotides against 40 mouse ubiquitin E3 enzymes were pre-designed by Qiagen and handled as instructed. Two different siRNA oligonucleotides against each gene were included in the initial screen. 10 pmol of siRNA oligonucleotides and 0.25 μl of Lipofectamine2000 were pre-incubated in a 0.1% gelatin-coated 96-well plate in 20 μl of OPTIMEM for 15 min at room temperature. The D3 mouse ES cells were trypsinized and seeded at 15,000 cells per well in 80 μl of ES cell medium on top of the siRNA mixture. Fresh medium was added to the cells the next day and the morphology of ES cell colonies were examined using bright-field microscopy at 48 h post transfection. Hit validation was performed with additional siRNAs that were purchased from two distinct vendors (Qiagen, Dharmacon) and that target different sites of the *Cul3* mRNA. Knockdown efficiency was tested by qRT–PCR and immunoblot.

Rescue of *Cul3*-siRNA phenotype in mouse ES cells by Matrigel and collagen IV. D3 mouse ES cells were grown on tissue culture dishes coated with gelatin (negative control), growth-factor-depleted Matrigel (BD Biosciences, catalogue no. 356231), or purified collagen IV (BD Biosciences, catalogue no. 354233). Matrigel and collagen IV were applied at 10 μg cm^{-2}. CUL3 was depleted 24 h later using our standard siRNA transfection protocol, and mouse ES cell morphology was analysed by confocal microscopy against integrin β1, actin and DNA.

Drug treatments of CUL3-depleted cells. To study the synthetic lethal effect of SRC-inhibition with CUL3 knockdown, we treated wild-type and CUL3-depleted D3 mouse ES cells with 0, 25, 50 or 100 nM of dasatinib for 18 h before the phenotypes were analysed by light microscopy.

To study the effect of RHO-inhibition on CUL3 knockdown, CUL3-depleted D3 mouse ES cells were treated with ROCK inhibitor Y27632 at 10 μM for 24 h before phenotype analysis. Alternatively, RHOA was co-depleted using specific siRNAs.

Cell cycle analysis. To assess the division rate of CUL3-depleted mouse ES cells, we treated cells with control, *Cul3*-, or *Ube2C*/*Ube2S*-siRNA and seeded at 3×10^5 cells per well in gelatin-coated six-well plates. The specificity of *Ube2S*- and *Ube2C*-siRNAs was tested before[40]. The cells were trypsinized at 2, 3 and 4 days post transfection and counted by haemocytometer.

ES cell differentiation analysis. To differentiate mouse ES cells into embryoid bodies (EB), we trypsinized undifferentiated D3 mouse ES cells, washed once with leukaemia inhibitory factor-free ES cell media, and seeded the cells at 2×10^6 cells per dish onto 10-cm Corning Ultra-Low-Attachment Dishes (Corning catalogue no. 3262) containing 10 ml of ES cell medium without leukaemia inhibitory factor. After 24 h, the cells were dissociated from the plate by gentle pipetting of the medium and collected in a 15-ml Falcon tube by centrifugation. The supernatant was aspirated off and the cells were re-seeded onto 10-cm Corning Ultra-Low-Attachment Dishes containing fresh ES cell medium without leukaemia inhibitory factor. Medium was changed every other day for a total of 6 or 9 days. Total RNA of ES cells and EB samples was extracted using TRIzol (Invitrogen, catalogue no. 15596-026) and chloroform. The expression of pluripotent markers and BTB genes at various time points during differentiation was analysed using quantitative real-time PCR.

As a complementary experiment, D3 mouse ES cells were treated with control or *Oct4* siRNA. 48 h after transfection, cells were collected and total RNA was extracted using TRIzol as above. The expression of pluripotent markers, tissue specific genes and BTB genes in control and OCT4-depleted cells were analysed using qRT–PCR.

Quantitative real-time PCR analysis. We used TRIzol (Invitrogen, catalogue no. 15596-026) and chloroform to extract total RNA from cells. The first-strand cDNAs were synthesized by using RevertAid first strand cDNA synthesis kit (Fermentas, catalogue no. K1621). Gene-specific primers for qRT–PCR were designed by using NCBI Primer-Blast. The quantitative RT–PCR reaction was done with the Maxima SYBR Green/Rox qPCR system (Fermentas, catalogue no. K0221).

Identification of CUL3–KLHL12 substrates. To identify CUL3–KLHL12 substrates, we generated a doxycycline-inducible human KLHL12–3×Flag stable cell line using the Flp-In T-REx 293 Cell Line system (Invitrogen). As controls, we generated stable cell lines expressing other BTB proteins including KLHL9. KLHL12–3×Flag and KLHL9–3×Flag expression was induced in 30 × 15 cm plates by 1 μg ml^{-1} of doxycycline for 48 h, and cells were collected by centrifugation and lysed by douncing 40 times in PBS+0.1%NP40. The cell lysate was cleared by centrifugation and then subjected to anti-Flag M2 affinity gel (Sigma, catalogue no. A2220-5mL) at 4 °C for 4 h on a rotator. Immunoprecipitations were eluted by 300 μl of 200 μg ml^{-1} 3×Flag peptide (Sigma, catalogue no. F4799-4MG) in PBS. The elution was repeated three times for 1 h at room temperature. Eluates were pooled, concentrated to 100 μl using Amicon Ultra-0.5, Ultracel-10 Membrane (Millipore, catalogue no. UFC501008) and run on a SDS–PAGE gel. The gel was stained by SimplyBlue SafeStain (Invitrogen, catalogue no. LC6060), and specific gel bands were cut out and sent for mass spectrometry analysis by the Vincent J. Coates Proteomics/Mass Spectrometry Laboratory at UC Berkeley.

Immunoprecipitation of endogenous protein complexes. To confirm the interaction of endogenous proteins, we lysed HeLa cells or D3 mouse ES cells by freeze-thaw twice in 20 mM HEPES buffer pH 7.5, 5 mM KCl, 1.5 mM $MgCl_2$, 1× protease inhibitor cocktail (Roche). Specific antibodies against CUL3, SEC13 or SEC31 conjugated to protein G agarose beads were added to the cleared cell lysate and incubated at 4 °C for 4 h. Protein complexes were eluted with gel-loading buffer at 95 °C. Endogenous proteins in complexes were detected by immunoblot using specific antibodies against CUL3, SEC13, SEC31 or KLHL12.

To detect ubiquitylation of endogenous COPII components, we incubated HeLa cell extract with pre-immune serum or antibody against SEC13 conjugated to protein G agarose beads at 4 °C for 4 h. Protein complexes were eluted with SDS gel-loading buffer at 95 °C. Ubiquitylated proteins in the complex were detected by immunoblot against ubiquitin.

***In vitro* protein interaction assays.** To dissect the KLHL12 and SEC31A interaction, we coupled 20 μg recombinant MBP–KLHL12, various mutants or MBP as a control to 15 μl amylose resin by incubating at 4 °C for 1 h. CUL3, SEC31A and mutants were expressed from pCS2 and labelled with [^{35}S]-Met using TnT Sp6 Quick Coupled Trsnc/trans Syst (Promega, catalogue no. L2080). The labelled CUL3 or SEC31A were incubated with MBP-KLHL12 or mutants at

4 °C for 3 h. Beads were washed four times with TBST and twice with TBS, and incubated in SDS loading buffer at 95 °C. Samples were run on SDS–PAGE and results were visualized by autoradiography.

***In vitro* ubiquitylation assays with CUL3–KLHL12.** CUL3/RBX1 was conjugated to NEDD8 at 30 °C for 1 h with the following conditions: 2.5 mM Tris/HCl pH 7.5, 5 mM NaCl, 1 mM $MgCl_2$, 1 mM DTT, 1× energy mix[40], 1 μM APPBP1–UBA3, 1.2 μM UBC12, 4 μM CUL3/RBX1, and 60 μM NEDD8. For *in vitro* ubiquitylation of SEC31A, we set up a 10 μl reaction as follows: 2.5 mM Tris/HCl pH 7.5, 5 mM NaCl, 1 mM MgCl2, 1 mM DTT, 1× energy mix, 100 nM UBA1, 1 μM UBCH5C, 1 μM CUL3∼NEDD8/RBX1, 1 μM KLHL12, 150 μM ubiquitin, 0.05 μg SEC13/31A. The reaction was carried out at 30 °C for 1 h and stopped by adding SDS gel loading buffer.

***In vivo* ubiquitylation assays with CUL3–KLHL12.** 293T cells grown in 10-cm dishes were transfected with pCS2-HA-Sec13/31A, pCS2-His-ubiquitin, pcDNA5-Klhl12-FLAG, pcDNA4-Cul3-FLAG, or pcDNA4-$Cul3^{N250}$-FLAG, as indicated, using calcium phosphate. 24 h later, 1 μM MG132 was added and cells were incubated overnight. Cells were harvested with gentle scraping and resuspended in 1 ml buffer A (6 M guanidine chloride, 0.1 M Na_2HPO_4/NaH_2PO_4 and 10 mM imidazole, pH 8.0). Cells were lysed by sonication for 10 s and incubated with 25 μl Ni-NTA agarose at room temperature for 3 h. The beads were washed twice with buffer A, twice with buffer A/TI (1 volume buffer A and 3 volumes buffer TI), once with buffer TI (25 mM Tris-Cl, 20 mM imidazole, pH 6.8), and incubated in 60 μl SDS gel-loading buffer containing 300 mM imidazole and 50 mM β-mercaptoethanol at 95 °C. Samples were separated by SDS–PAGE and ubiquitylated SEC31A was detected by immunoblot using antibody against SEC31A.

To detect SEC31A ubiquitylation upon CUL3/KLHL12 depletion, we co-transfected 100 nM siRNAs against CUL3 or KLHL12 with pCS2-HA-Sec13/31A and pCS2-His-ubiquitin using calcium phosphate. The Ni-NTA purification was performed 48 h post transfection and SEC31A ubiquitylation was detected as described above.

Confocal microscopy. Cells were fixed in 4% paraformaldehyde and permeabilized with 0.5% Triton X-100 in 1× TBS, 2% BSA. Cells were incubated with primary antibodies against SEC31A, SEC13, SEC24C, ERGIC53, CD63, BiP (also known as HSPA5) or ubiquitin for 2 h and secondary antibodies (Invitrogen, Alexa Fluor 546 goat anti-rabbit IgG (H+L); Alexa Fluor 488 goat anti-mouse IgG (H+L); HOECHST 33342,) for 1 h at room temperature followed by extensive washing. Pictures were taken on Zeiss LSM 510 and 710 Confocal Microscope systems and analysed with LSM image browser and Imaris 3D imaging processing software.

Transmission electron microscopy. Mock- and KLHL12-transfected HeLa cells were grown to 70% confluence as a monolayer on an Aclar sheet (Electron Microscopy Sciences). The cells were fixed for 30 min in 0.1 M cacodylate buffer, pH 7.2, containing 2% glutaraldehyde, and subsequently washed with buffer before post-fixation with 1% osmium tetroxide on ice. This was followed by staining with 1% aqueous uranyl acetate for 30 min at room temperature. For dehydration with progressive lowering of temperature, each incubation period was 10 min, with exposure to 35% ethanol at 4 °C, to 50% ethanol and 70% ethanol at −20 °C, and 95%, and 100% ethanol at −35 °C. Cells were restored to room temperature in 100% ethanol before flat embedding in an Epon resin. Thin (70–100 nm) sections were collected on Formvar-coated 200-mesh copper grids and post-stained with 2% aqueous uranyl acetate and 2% tannic acid. The sections were imaged at 120 kV using a Tecnai 12 Transmission Electron Microscope (FEI).

For the purpose of immunolabelling, HeLa cells expressing Flag–KLHL12 or doxycycline-inducible 293T Trex Flag–KLHL12 stable cell lines were fixed in 2% paraformaldehyde and 0.5% glutaraldehyde and embedded in LR white resin. Fixation and infiltration were performed in a microwave oven (Pelco model 3450, Ted Pella). 70-nm thick sections were picked on 100-mesh nickel grids coated with Formvar film and carbon, incubated in blocking buffer (5% BSA, 0.1% fish gelatin, 0.05% Tween 20 in PBS) for 30 min, and followed by incubation with anti-Flag antibody at a dilution of 1:40 for 1 h. Goat anti-mouse IgG conjugated with 10-nm gold (BD Biosciences) was used as the secondary antibody at a dilution of 1:40 for 1 h. Sections were post stained in 2% uranyl acetate for 5 min.

Gene expression analysis by microarray. To compare gene expression profiles of wild-type mouse ES cells versus CUL3-depleted mouse ES cells, we transfected D3 mouse ES cells with control or *Cul3*-siRNA, followed by growth on gelatin-coated six-well plates. 48 h later, total RNA was extracted by TRIzol and chloroform, and further purified using RNeasy Mini Kit (Qiagen, catalogue no. 74104). Microarray analysis was performed by the Functional Genomics Laboratory (UC Berkeley) using Affymetrix Mouse 430A 2.0 chip.

Analysis of collagen export from cells. IMR-90 human lung fibroblasts grown on 100-mm dishes in DMEM/10% FBS were transfected with Flag–KLHL12, Flag–KLHL12(FG289AA), Flag–KEAP1 and pcDNA5-flag using nucleofection kit R (bought from Lonza) as described in the manufacturer's protocol and plated on six-well plate with 25-mm coverslips. When indicated, co-transfections with 2 μg each of Flag–KLHL12 and dominant-negative CUL3 were performed. Dialysed 10% FBS media was used for ascorbate free transfections. Brefeldin A (Sigma) was used at a concentration of 2.5 mg ml^{-1} and cells were incubated for 30 min. MG132 was used at 20 μM for 2 h, chloroquine was used at 200 μM for 1 h. Media was collected the next day and cells on coverslips were fixed with 3% paraformaldehyde for 30 min and remaining cells on a plate were used to prepare lysates. Cells on coverslips were permeabilized with 0.1% Triton for 15 min at room temperature followed by blocking with 1%BSA for 30 min. Primary antibodies used were polyclonal anti-procollagen (LF-67,diluted 1:1,000) and anti-Flag (diluted 1:200). Secondary antibodies were Alexa Fluor 546 donkey anti-rabbit IgG and Alexa Fluor 488 goat anti-rabbit IgG (diluted 1:200). After staining cells with appropriate primary and secondary antibodies, we fixed coverslips on slides using mounting reagent containing DAPI. Images were analysed with a Zeiss LSM710 confocal microscope and captured with Zen10 software. Merges of images were performed with ImageJ and LSM image Browser. Media collected from six-well plates was normalized with respect to lysate protein concentration estimated using BCA method. Media and lysates of each reaction were checked by immunoblot analysis. Tubulin was used as loading control for lysates. Ascorbate chase experiments were done by adding ascorbate (0.25 mM ascorbic acid and 1 mM asc-2-phosphate) to KLHL12-transfected cells, followed by incubation for 5, 10, 30 and 60 min.

A human fibrosarcoma cell line (HT1080) stably transfected with proalpha1(1) was used for CUL3 knockdowns. *Cul3*- and *Klh12*-shRNAs targeting two different regions in both genes were cloned into pSuperGFP and transfected using Lipofectamine 2000. pSuper GFP was used as negative control. Cells were grown on 25-mm coverslips in six-well plates and fixed 2 days post transfection. Collagen staining was done using LF-67 (1:1,000) and endoplasmic reticulum was stained with anti-PDI (1:1,000) antibody. Fibronectin and EGFR were stained in parallel experiments. Fibronectin expression was induced in HT1080 using 1 μM dexamethasone before CUL3 knockdowns. Endoplasmic reticulum retention or secretion was scored in cells expressing GFP shRNAs. Cells without GFP shRNAs and transfected with pSUPER GFP were quantified as well. Images were taken on a Zeiss LSM 710 confocal microscope and visualized with LSM image browser. Lysates were prepared from remaining cells on six-well plates and checked for knockdown efficiency.

siRNA oligonucleotides used in this study. RNA interference oligonucleotides: mCul3 #1, GAAGGAATGTTTAGGGATA; mCul3 #2, GGAAGAAGATGCAG CACAA; mCul3 #3, GGTGATGATTAGAGACATA; mCul3 #4, CAACTTTCT TCAAACACTA; mCul3 #5, CATTATTTATTGATGATAA; mUBA3, CGTTTG AAGCAGAGAGAAA; mKlhl12, CCTTGAGAGTGGAGCAGAA; hKlhl12, CCAAAGACATAATGACAAA; mKBTBD8, GAACATGAGCAGAGTGAAA; mOct4, AGGCAAGGGAGGTAGACAA; hSec31, CCTGAAGTATTCTGAT AAA; mSec13 (pool of 4 oligonucleotides), CCATGTGTTTAGTAATTTA, GGCAATATGTGGTCACCTA, GCTGAAAGTATTCATGTAA and GGAAC AAATGACTATTATT; mCdc42 (pool of 4 oligonucleotides), GATCTAATT TGAAATATTA, GGATTGAGTTCCTAATTAA, AGAGGATTATGACAGAC TA and AAATCAAACTAAAGATTAA; mBcar1/CAS (pool of 4 oligonucleotides), GACTAATAGTCTACATTTA, GGAGGTGTCTCGTCCAATA, CTATGACA ATGTTGCTGAA and GGGCGTCCATGCTCCGGTA; mSrc (pool of 4 oligonucleotides), CCCTTGTGTCCATATTTAA, CCACGAGGGTTGCCATCAA, CA GACTTGTTGTACATATT and GCAACAAGAGCAAGCCCAA; mRhoG (pool of 4 oligonucleotides), GGTTTACCTAAGAGGCCAA, GCTGTGCCTTAAG GACTAA, GCACAATGCAGAGCATCAA and GGCGCACCGTGAACCTA AA; mRhoA (pool of 4 oligonucleotides), GGATTTCCTAATACTGATA, GAAAGTGTATTTGGAAATA, AGCCCTATATATCATTCTA, CGTCTGCCA TGATTGGTTA; mRac1 (pool of 4 oligonucleotides), GGTTAATTTCTGTCA AACA, GCGTTGAGTCCATATTTAA, GCTTGATCTTAGGGATGAT and GGAGTAATTCAACTGAATA; mCdh1/E-cadherin (pool of 4 oligonucleotides), GGAGGAGAACGGTGGTCAA, CGCGGATAACCAGAACAAA, CCATGTTT GCTGTATTCTA and GGGACAATGTGTATTACTA; mIqgap1 (pool of 4 oligonucleotides), ACATGATGATGATAAACAA, GGTTGATTTCACAGAAGAA, GTATAAATTTATTTCTTAA and GGTGGATCAGATTCAAGAA; mCul1 (pool of 2 oligonucleotides), GCATGATCTCCAAGTTAAA and CGTGTAATC TGCTATGAAA; mCul2 (pool of 2 oligonucleotides), GCGCTGATTTGAAC AATAA and CCAGAGTATTTATATCTAA; mCul4a (pool of 2 oligonucleotides), GTGTGATTACCATAATAAA and CCAGGAAGCTGGTCATCAA; mCul5 (pool of 2 oligonucleotides), CCCTCATATTTACAGCAAA and ACATGAAGTT TATAATGAA; mCul7 (pool of 2 oligonucleotides), GCATCAAGTCCGTTAA TAA and GGATGTGATTGATATTGAA.

39. Geddis, A. E. & Prockop, D. J. Expression of human *COL1A1* gene in stably transfected HT1080 cells: the production of a thermostable homotrimer of type I collagen in a recombinant system. *Matrix* **13,** 399–405 (1993).
40. Williamson, A. *et al.* Identification of a physiological E2 module for the human anaphase-promoting complex. *Proc. Natl Acad. Sci. USA* **106,** 18213–18218 (2009).

doi:10.1038/nature10822

Supplementary Figures

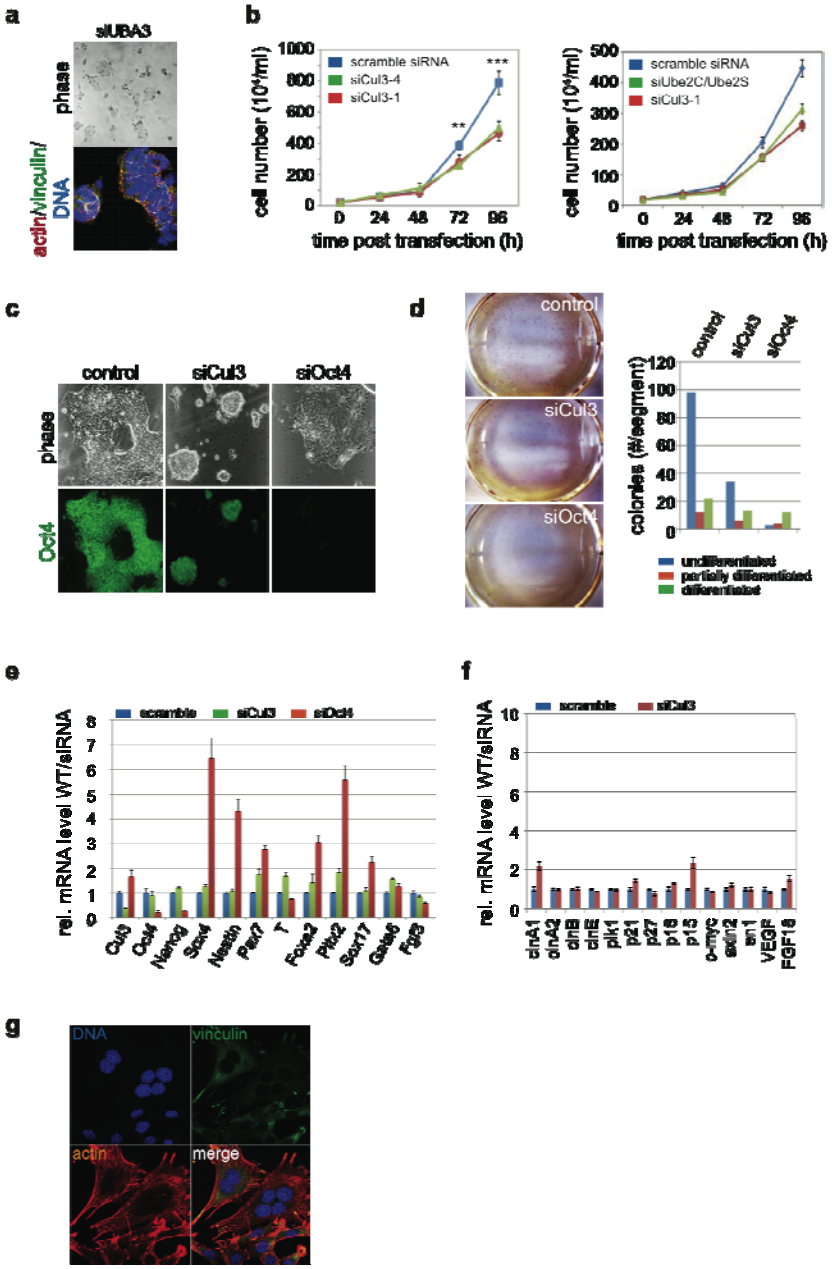

Figure S1: Cul3 is required for mESC division in culture. a. Depletion of UBA3 leads to mESC clustering and compaction. D3 mESCs grown on gelatin were treated with

siRNAs against UBA3 and analyzed by phase (upper panel) or confocal microscopy with staining against actin (red), vinculin (green), and DNA (blue; lower panel). **b.** Cul3 is required for rapid mESC proliferation. *Left panel:* D3 mESCs were treated with control siRNA or siRNAs against Cul3 and proliferation was monitored by cell counting in three independent experiments; the error bars represent the standard deviation of the mean. *Right panel:* depletion of Cul3 is compared to depletion of Ube2S and Ube2C, the E2s of APC/C. The APC/C is required for cell division, underscoring the strong phenotype of the Cul3 knockdown. **c.** Cul3 is not required for maintaining pluripotency. D3 mESCs were treated with siRNAs against control, Cul3, or Oct4. Differentiation was followed by phase (upper panel) or confocal microscopy staining for Oct4 (lower panel). **d.** Cul3 is not required for maintaining pluripotency of mESCs, as judged by expression of alkaline phosphatase. D3 mESCs were treated with siRNAs against control, Cul3, or Oct4, and cell number, alkaline phosphatase staining, and differentiation status as judged by cell morphology were monitored. Depletion of Cul3 reduces cell number, but not alkaline phosphatase staining or differentiation status. **e.** Depletion of Cul3 does not induce expression of differentiation markers. D3 mESCs were treated with control siRNAs or siRNAs targeting Cul3 or Oct4. The expression of established differentiation markers was monitored by qRT-PCR in three independent experiments. The error bars represent the standard deviation of the mean. **f.** Depletion of Cul3 does not lead to gross misexpression of cell cycle genes or Wnt-target genes, as determined by qRT-PCR in WT- and siCul3-treated mESCs. Error bars denote the standard deviation from three independent experiments. **g.** Depletion of Cul3 in mouse NIH3T3 fibroblasts results in multinucleation, but not cell compaction or clustering. NIH3T3 cells were treated with siRNAs against control or Cul3 and analyzed by phase (upper panel) or confocal microscopy against actin (red), vinculin (green) or DNA (blue). Examples of the frequent multinuclear cells observed in the absence of Cul3 are shown.

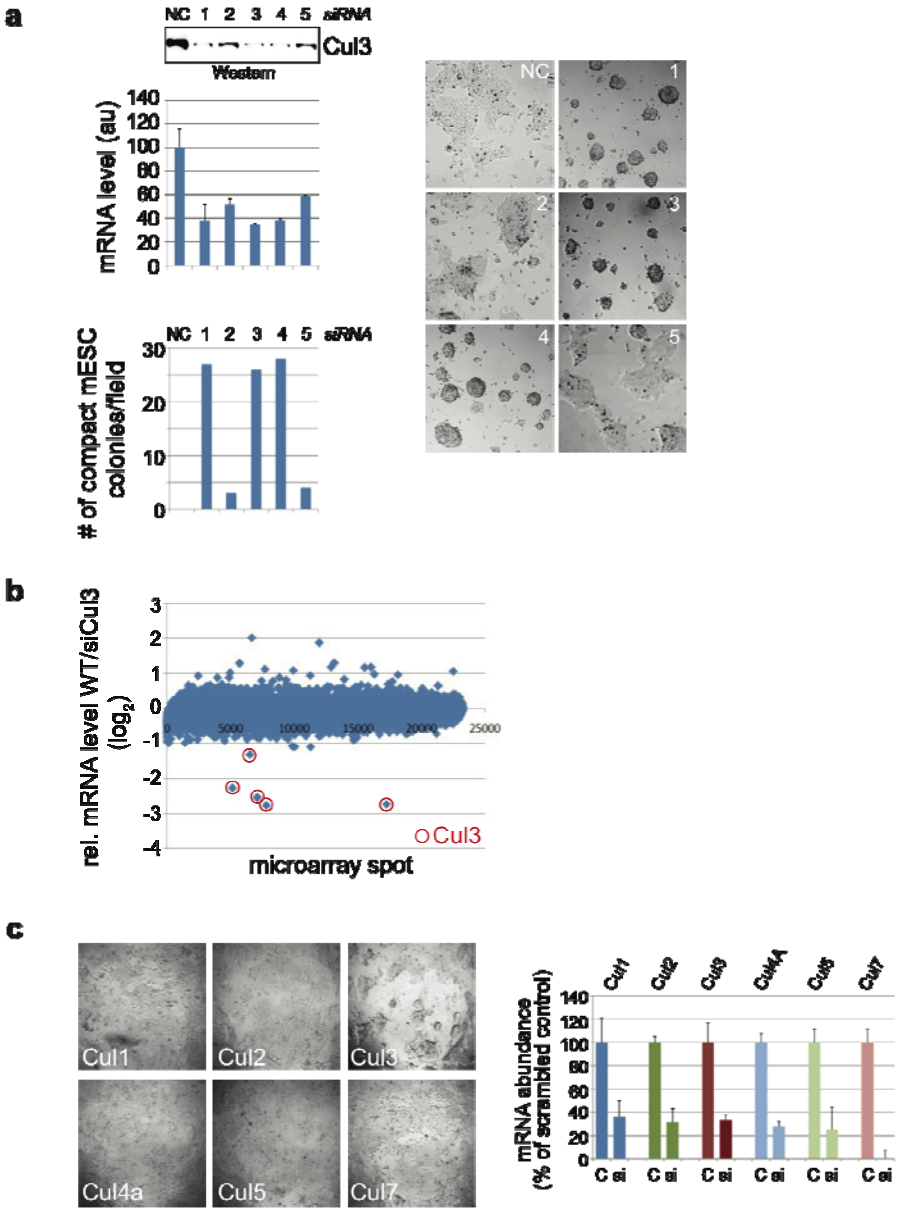

Figure S2: Specific effects of Cul3 depletion in mESCs. a. Multiple siRNAs targeting the Cul3 open reading frame result in mESC clustering and compaction. D3 mESCs were grown on gelatin and transfected with control siRNA or five siRNAs targeting

distinct sequences in the Cul3 open reading frame. Knockdown efficiency was measured by immunoblot (upper left panel) and qRT-PCR (lower left panel), with the error bars representing the standard deviation of three independent experiments. mESC clustering monitored by phase microscopy (right panels) revealed a clear correlation between knockdown efficiency and strength of phenotype. **b.** Specific depletion of Cul3 in mESCs. D3 mESCs were transfected with control siRNA or siRNA against Cul3 and mRNA levels were analyzed globally by microarray analysis. The only significantly reduced mRNA was Cul3 (microarray spots targeting Cul3 are encircled in red). **c.** Depletion of Cul3, but not of any other cullin, results in mESC clustering. D3 mESCs were transfected with siRNAs targeting the indicated mouse cullins and analyzed for mESC clustering by phase microscopy. Knockdown efficiency was controlled by qRT-PCR (right panel). Error bars denote the standard deviation from three independent experiments.

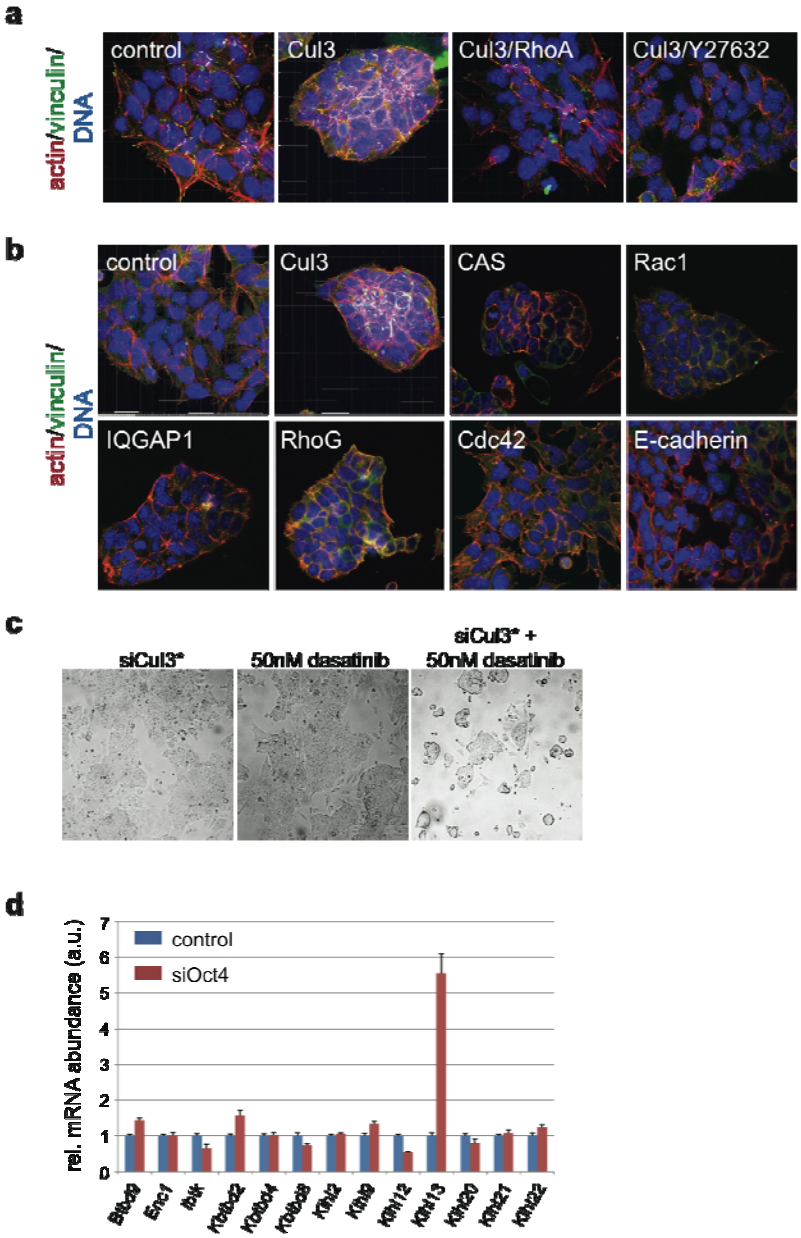

Figure S3: Cul3 is required for integrin-signaling in mESCs grown on gelatin. a. mESC clustering and compaction of Cul3-depleted mESCs is rescued by inhibition of RhoA-signaling. D3 mESCs grown on gelatin were treated with siRNAs against control, Cul3, or Cul3 and RhoA. In the last experiment, Cul3-depleted mESCs were treated with

ROCK1-inhibitor Y27532. mESC clustering and compaction were monitored as before by confocal microscopy against actin (red), vinculin (green) or DNA (blue). **b.** Inhibition of integrin signaling phenocopies loss of Cul3 from mESCs. D3 mESCs plated on gelatin were treated with siRNAs targeting the indicated proteins (white inserts) and analyzed for cell compaction by actin- (red), vinculin- (green), and DNA-staining. **c.** Cul3 and Src kinase show genetic interaction. D3 mESCs were transfected with an siRNA against Cul3 that leads to its partial depletion and no cell clustering or compaction; alternatively, D3 mESCs were treated with 50nM of the Src-inhibitor dasatinib, which does not have a phenotype either. However, when both treatments were combined, mESC clustering was observed, as judged by phase microscopy. **d.** Expression of Cul3-adaptors is regulated during differentiation. D3 mESCs were transfected with siRNAs against control or Oct4 and the relative mRNA abundance of Cul3-adaptors with BTB-domains was measured by qRT-PCR. The expression of Klhl12 is downregulated in this experiment, as well as upon differentiation of mESCs through removal of LIF (see Fig. 2). Error bars denote the standard deviation from three independent experiments.

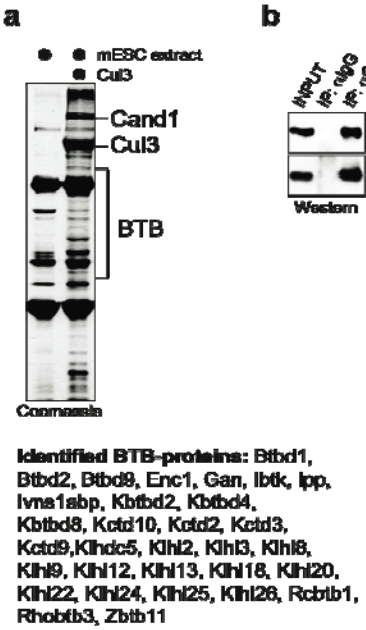

Figure S4: Klhl12 is a substrate adaptor for Cul3 in mESCs. a. Immobilized ^{FLAG}Cul3 was incubated with extracts of D3 mESCs, and specific binding partners were identified by mass spectrometry. **b.** Klhl12 binds Cul3 in mESCs. Lysates of D3 mESCs were treated with αCul3- or control-antibodies and Klhl12 was detected by immunoblotting. Input corresponds to ~10% of the lysates used for the immunoprecipitation.

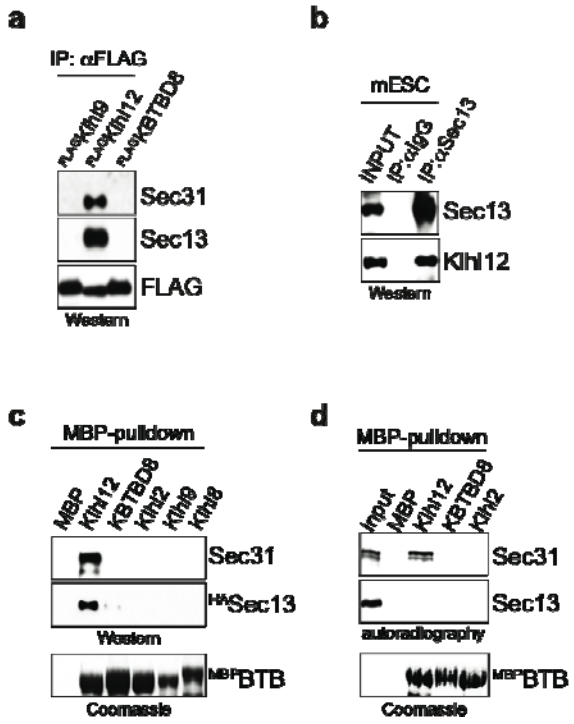

Figure S5: Klhl12 interacts with Sec31. a. Klhl12 binds the Sec13/Sec31 heterotetramer in cells. ^{FLAG}Klhl9, ^{FLAG}Klhl12, or ^{FLAG}Kbtbd8 were immunoprecipitated from lysates of stable 293T cell lines by αFLAG-agarose, and co-purifying endogenous

Sec13 or Sec31 were detected by immunoblotting. **b.** Klhl12 interacts with Sec13 in mESCs. Endogenous Sec13 was precipitated from lysates of D3 mESCs with rabbit αSec13-antibodies, and co-purifying Klhl12 was detected by immunoblotting. Sec31 could not be detected in these experiments due to a cross-reactivity of the antibody with mouse cell lysates. Control experiments were performed using pre-immune rabbit IgGs. **c.** Klhl12 directly interacts with Sec13/31. MBP or a series of ^{MBP}BTB-proteins, including ^{MBP}Klhl12, were coupled to amylose resin and incubated with recombinant Sec13/31 purified from insect cells. Binding of Sec13/31 was monitored by immunoblotting. **d.** Klhl12 binds Sec31. Purified ^{MBP}BTB-proteins, including ^{MBP}Klhl12, were immobilized on amylose resin and incubated with ^{35}S-labeled Sec31 or Sec13 synthesized by *in vitro* transcription/translation. Bound proteins were detected by autoradiography.

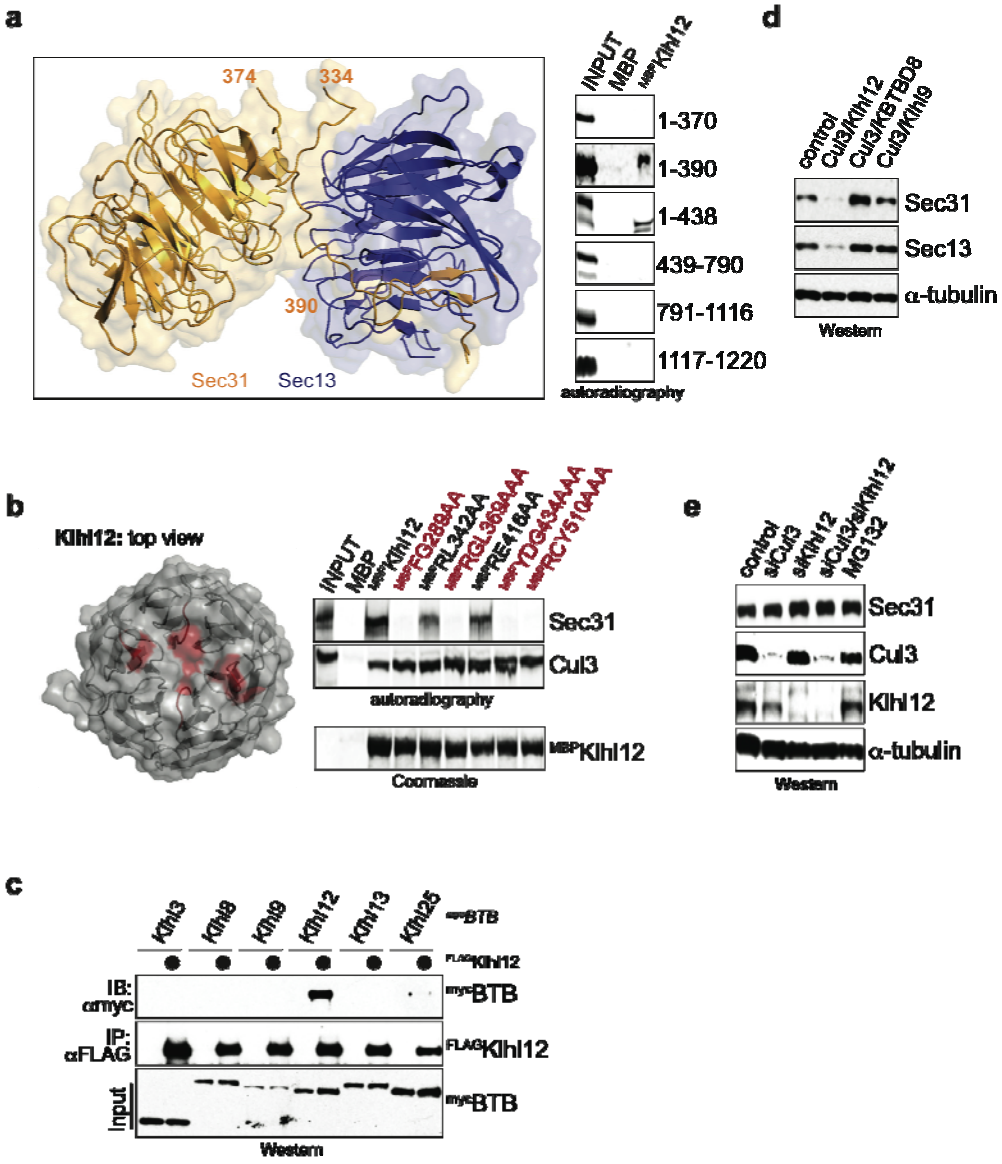

Figure S6: Characterization of the Sec31/Klhl12-interaction. a. Klh12 recognizes residues in the N-terminal domain of Sec31. Binding of ^{35}S-labeled Sec31-truncations to ^{MBP}Klhl12 or MBP was monitored by autoradiography. Klhl12 requires residues 370-390 for binding, which are located in the loop between the Sec31-WD40-repeat and the

Sec13-binding site (left panel; Sec31 gold, Sec13 blue; pdb 2PM9). **b.** Klhl12 utilizes its Kelch-repeats to bind Sec31. ^{MBP}Klhl12 and mutants in the Kelch-repeats were immobilized on amylose resin and incubated with ^{35}S-labeled Sec31 or Cul3, respectively. Binding was monitored by autoradiography. Klhl12-mutants defective in Sec31-, but not Cul3-binding, are shown in red. The left panel shows the structure of the Kelch-repeats in Klhl12 (pdb 2VPJ), with residues required for Sec31-binding highlighted in red. **c.** Klhl12 dimerizes in vivo. 293T cells were transfected with ^{FLAG}Klhl12 and ^{myc}BTB proteins as indicated. ^{FLAG}Klhl12-complexes were precipitated on αFLAG-agarose and analyzed for co-purifying proteins by αmyc-Western. Dimerization of Klhl12 could explain the dominant negative effect of mutant Klhl12 on Sec31 ubiquitination. **d.** Overexpression of Cul3 and Klhl12 can induce Sec31-degradation in cells. The abundance of ^{HA}Sec31 that was co-transfected with the indicated Cul3 and BTB-proteins was determined by immunoblot using specific αSec31-antibodies. **e.** Endogenous Cul3 or Klhl12 do not regulate Sec31-levels in cells. Cul3 and Klhl12 were depleted from HeLa cells using specific siRNAs as indicated; the proteasome was inhibited by addition of MG132. The abundance of Sec31 was measured using immunoblot and specific αSec31-antibodies.

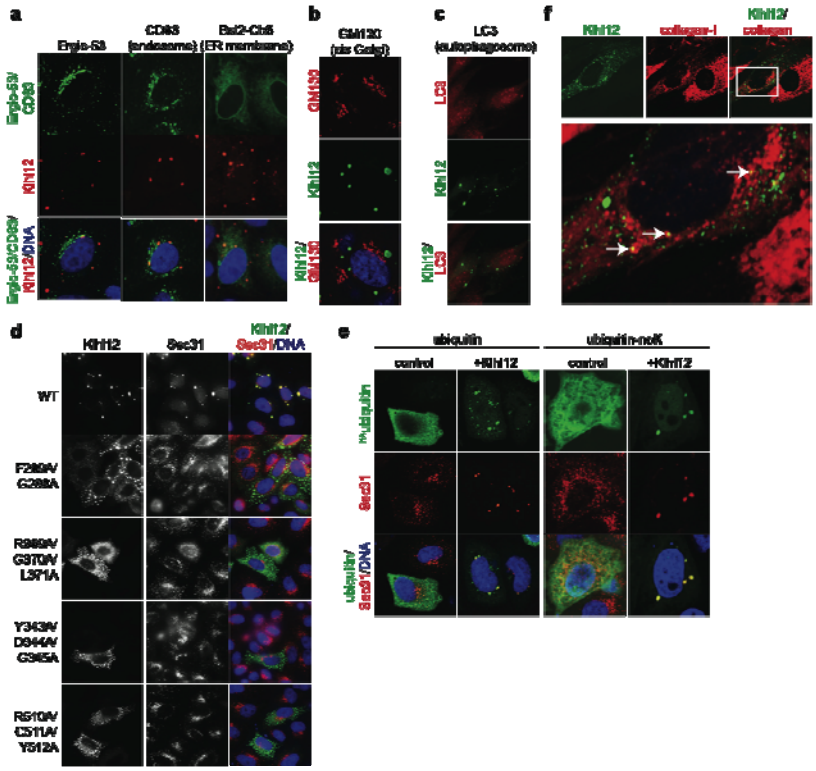

Figure S7: Cul3^{Klhl12} induces formation of large COPII coats. a. Ergic-53, CD63 (endosomal marker), and Bcl2-Cb5 (ER-marker) do not co-localize with Klhl12-induced large structures. HeLa cells were transfected with ^{FLAG}Klhl12 and the localization of Klhl12 (red), marker proteins (green), and DNA (blue) were analyzed by confocal

microscopy. In the last panel, GFP-Bcl2-Cb5 was co-transfected with Klhl12. **b.** Klhl12 does not co-localize with GM130, a cis-Golgi protein, and Klhl12-expression does not alter the structure of the cis-Golgi, as seen by confocal microscopy against ^{FLAG}Klhl12 (green), GM130 (red), and DNA (blue). **c.** Klhl12 (green) does not induce formation of autophagosomes, as seen by staining for LC3 (red). **d.** Sec31-binding deficient Klhl12 mutants do not induce formation of large COPII-structures. HeLa cells were transfected with Klhl12 or the indicated mutants in the Sec31-binding interface, and the localization of Klhl12 (green), Sec31 (red), and DNA (blue) was analyzed by confocal microscopy. **e.** Klhl12-dependent COPII-structures are enriched for ubiquitin. HeLa cells were transfected with ^{HA}ubiquitin or a ubiquitin mutant lacking all lysine residues, and ^{FLAG}Klhl12, and the localization of ubiquitin (green), Sec31 (red), and DNA (blue) was analyzed by confocal microscopy. **f.** Collagen-I (red) and Klhl12 (green) partially co-localize in IMR90-cells 10min after addition of ascorbate to the culture medium.

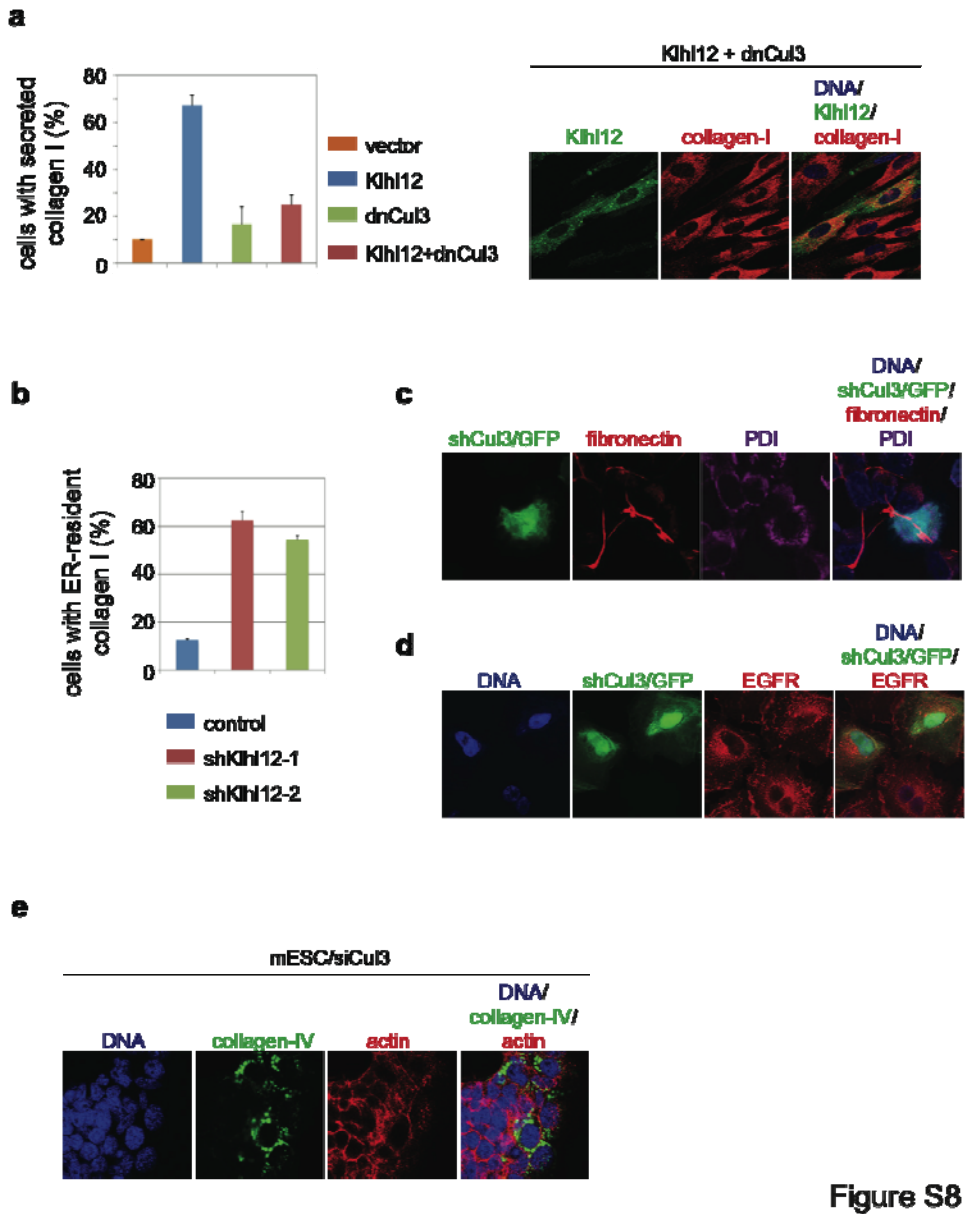

Figure S8: Cul3^{Klhl12}-dependent ubiquitination is required for collagen secretion. a. Cul3-dependent ubiquitination is required for the Klhl12-dependent increase in collagen secretion from IMR90 cells. IMR90 cells were transfected with ^{FLAG}Klhl12, and intracellular levels of collagen-I were monitored by confocal microscopy. To interfere with

ubiquitination, dominant negative (dn) Cul3 (Cul31-250) was expressed in parallel. Error bars denote the standard deviation from three independent experiments. **b.** Klh12 is required for collagen secretion in HT1080 cells. HT1080 cells constitutively synthesizing and secreting collagen-I were transfected with two independent shRNAs against Klhl12 and the number of cells with intracellular pools of collagen-I was determined by confocal microscopy. Error bars denote the standard deviation from three independent experiments. **c.** Cul3 is not required for export of fibronectin. HT1080 cells were transfected with shRNA-1 against Cul3 and levels of intra- and extracellular fibronectin were determined by confocal microscopy. **d.** Cul3 is not required for the proper localization of EGF receptor, as determined by confocal microscopy. Both untransfected HT1080 cells and those cells that were transfected with shRNAs against Cul3 show identical EGFR localization. **e.** Intracellular accumulation of collagen-IV in mESCs in not a secondary consequence of cell clustering. mESCs were plated at low density and stained for collagen-IV (green), actin (red), and DNA (blue). Cells at the edges of clusters were analyzed for intracellular collagen-IV.

Supplementary Methods

Plasmids, protein, antibodies

Human Cul3 and Klhl12 were cloned into pcDNA4 and pcDNA5 vectors for expression in mammalian cells. Cul3, Sec31A and Sec13 were also cloned into pCS2 vector for IVT/T and expression in mammalian cells. pcDNA4-Cul3^{N250} contains the first cullin repeat of the N-terminal Cul3 (1-250aa) which is sufficient for binding BTB proteins, but not Rbx1 and serves as a dominant negative for Cul3/BTB-mediated ubiquitination. The Klhl12 mutants FG289AA, RL342AA, RGL369AAA, RE416AA, YDG434AAA and RCY510AAA were made by site-directed mutagenesis.

Cul3 and Rbx1 were cloned into pFastBac, co-expressed in Sf9 ES insect cells using the Bac-to-Bac baculovirus expression system (Invitrogen) and purified as a complex by Ni-NTA agarose (Qiagen). Similarly, the Sec31A/Sec13 heterodimer and UBA1 were purified from Sf9 ES insect cells. UbcH5c and Ubc12 were cloned into pQE vector and purified from BL21(DE3) bacterial cells. Ubiquitin was cloned into pET and pCS2 vector with a N-terminal 6xHis tag. The pET-His-ubiquitin was used for bacterial purification whereas pCS2-His-ubiquitin was expressed in mammalian cells. Wildtype ubiquitin, APPBP1-UBA3 and NEDD8 were purchased from Boston Biochem.

To purify recombinant Klhl12 for ubiquitination assays, we expressed pMAL-TEV-Klhl12-his and pMAL-TEV-Klhl12^{FG289AA}-his in BL21(DE3) cells, purified the proteins on amylose resin, cleaved them by TEV protease, and re-purified them on Ni-NTA agarose. WT-Klhl12 and mutants were also cloned into pMAL vector and purified as MBP-tagged proteins for in-vitro protein binding assays.

All shRNAs were cloned in pSuper-GFP neo vector (from Oligoengine) into BglII and XhoI sites. The GFP-Bcl2-Cb5 construct, a fusion between Bcl2 and cytochrome b5, was purchased from Clontech.

We raised mouse monoclonal antibodies against human Klhl12 and human Klhl13. Both antibodies are available at Promab Biotechnologies (cat. # 30058 and # 30067). We also raised antibodies against Sec13, Sec24C, and Sec24D. Other antibodies used in this study are: Cul3 (Bethyl Laboratories, cat. # A301-109A), Sec31A (BD Biosciences, cat. # 612350), Collagen IV (Abcam, cat. # ab19808), anti-FLAG (Sigma, cat. #F3165, #F7425), Ubiquitin (Santa Cruz, cat. # sc-8017, P4D1), Rhodomine phalloidin (Invitrogen, cat. # R415), PDI (1D3) (Assay Designs, cat. #SPA-891), anti LC-3 (Sigma, Cat # L-7543), anti-alpha tubulin (DM1A, Abcam, Cat # ab7291), anti-fibronectin (Abcam, ab2413), anti-GM130 (BD Biosciences, cat. # 610822), and anti-EGFR (Ab12, Neomarkers, MS-400P1). LF-67 (Anti sera for Type I procollagen) was obtained as a generous gift from Dr. Larry Fisher.

Cell culture

The D3 mouse embryonic stem cells (mESC) were maintained in ESC medium containing 15% FBS, 1x sodium pyruvate, 1x NEAA, 1mM β-ME and 1000u/ml LIF (Millipore, cat. # ESG1107) in GIBCO Dulbecco's Modified Eagle Medium, and grown on 0.1% gelatin-coated tissue culture plates. Hela cells, 293T cells, 3T3 cells and IMR90 cells were maintained in DMEM plus 10% FBS. Dialyzed FBS was bought from Hyclone. The doxycycline-inducible 293T Trex Klhl12-3xFLAG stable cell line was made with Flp-In™ T-REx™ 293 Cell Line system from Invitrogen. Stable cell lines expressing other BTB-proteins were generated accordingly. These cell lines were maintained with 10% TET(-) FBS, blasticidin and hydromycin B as instructed and expression was induced by 1ug/ml doxycycline.

Human lung fibroblasts IMR-90 cells were obtained from the Corielle Institute: NIA (National Institute on Aging) Aging Cell Repository. For generating procollagen

stable HT-1080cell lines, we cloned proalpha(1) into a pRMc/CMV-vector and selected for neomycin resistance [39]. This vector was provided as a generous gift by Neil Bulleid. Cells were kept in a 37°C incubator at 5%CO_2.

siRNA screen in mouse ES cells

siRNA oligos against 40 mouse ubiquitin E3 enzymes were pre-designed by Qiagen and handled as instructed. Two different siRNA oligos against each gene were included in the initial screen. 10pmol of siRNA oligos and 0.25ul of Lipofectamine2000 were pre-incubated in a 0.1% gelatin-coated 96-well plate in 20ul of OPTIMEM for 15min at room temperature. The D3 mESCs were trypsinized and seeded at 15000 cells/well in 80ul of ESC medium on top of the siRNA mixture. Fresh medium was added to the cells the next day and the morphology of ES cell colonies were examined using bright-field microscopy at 48h post transfection. Hit validation was performed with additional siRNAs that were purchased from two distinct vendors (Qiagen, Dharmacon) and that target different sites of the Cul3 mRNA. Knockdown efficiency was tested by qRT-PCR and immunoblot.

Rescue of Cul3-siRNA phenotype in mESCs by matrigel and collagen-IV

D3 mESCs were cultured on tissue culture dishes coated with gelatin (negative control), growth-factor depleted matrigel (BD Biosciences, cat# 356231), or purified collagen-IV (BD Biosciences, cat# 354233). Matrigel and collagen-IV were applied at 10$\mu g/cm^2$. Cul3 was depleted 24h later using our standard siRNA transfection protocol, and mESC morphology was analyzed by confocal microscopy against β1-integrin, actin, and DNA.

Drug treatments of Cul3-depleted cells

To study the synthetic lethal effect of Src-inhibition with Cul3 knockdown, we treated wildtype and Cul3-depleted D3 mESCs with 0, 25, 50, 100nM of dasatinib for 18h before the phenotypes were analyzed by light microscopy.

To study the effect of Rho-inhibition on Cul3 knockdown, Cul3-depleted D3 mESCs were treated with ROCK inhibitor Y27632 at 10uM for 24h before phenotype analysis. Alternatively, RhoA was co-depleted using specific siRNAs.

Cell cycle analysis

To assess the division rate of Cul3-depleted mESCs, we treated cells with control, Cul3-, or Ube2C/Ube2S-siRNA and seeded at $3x10^5$ cells/well in gelatin-coated 6-well plates. The specificity of Ube2S- and Ube2C-siRNAs was tested before [40]. The cells were trypsinized at 2, 3 and 4d post transfection and counted by hemocytometer.

ES cell differentiation analysis

To differentiate mouse ES cells into embryoid bodies (EBs), we trypsinized undifferentiated D3 mouse ES cells, washed once with LIF-free ESC media, and seeded the cells at $2x10^6$ cells/dish onto 10-cm Corning Ultra-Low-Attachment Dishes (Corning cat. # 3262) containing 10 ml of ESC medium without LIF. After 24h, the cells were dissociated from the plate by gentle pipetting of the medium and collected in a 15ml Falcon tube by centrifugation. The supernatant was aspirated off and the cells were re-seeded onto 10-cm Corning Ultra-Low-Attachment Dishes containing fresh ESC medium without LIF. Medium was changed every other day for a total of 6 or 9d. Total RNA of ESCs and EB samples was extracted using TRIzol (Invitrogen, cat. # 15596-026) and chloroform. The expression of pluripotent markers and BTB genes at various time points during differentiation was analyzed using quantitative real-time PCR.

As a complementary experiment, D3 mESCs were treated with control or Oct4 siRNA. 48h after transfection, cells were collected and total RNA was extracted using TRIzol as above. The expression of pluripotent markers, tissue specific genes and BTB genes in control and Oct4-depleted cells were analyzed using qRT-PCR.

Quantitative real-time PCR analysis

We used TRIzol (Invitrogen, cat. # 15596-026) and chloroform to extract total RNA from cells. The first-strand cDNAs were synthesized by using Revertaid first strand cDNA synthesis kit (Fermentas, cat. # K1621). Gene-specific primers for qRT-PCR were designed by using NCBI Primer-Blast. The quantitative RT-PCR reaction was done with the Maxima SYBR Green/Rox qPCR system (Fermentas, cat. # K0221).

Identification of Cul3^{Klhl12}-substrates

To identify Cul3^{Klhl12} substrates, we generated a doxycycline-inducible hKlhl12-3xFLAG stable cell line using the Flp-In™ T-REx™ 293 Cell Line system (Invitrogen). As controls, we generated stable cell lines expressing other BTB proteins including Klhl9. Klhl12-3xFLAG and Klhl9-3xFLAG expression was induced in 30x15cm-plates by 1ug/ml of doxycycline for 48h, and cells were collected by centrifugation and lysed by douncing 40 times in PBS+0.1%NP40. The cell lysate was cleared by centrifugation and then subjected to anti-FLAG M2 affinity gel (Sigma, cat. # A2220-5mL) at 4C for 4h on a rotator. Immunoprecipitations were eluted by 300ul of 200ug/ml 3xFLAG peptide (Sigma, cat. # F4799-4MG) in PBS. The elution was repeated three times for 1h at room temperature. Eluates were pooled, concentrated to 100ul using Amicon Ultra-0.5, Ultracel-10 Membrane (Millipore, cat. # UFC501008) and run on a SDS-PAGE gel. The gel was stained by SimplyBlue™ SafeStain (Invitrogen, cat. # LC6060), and specific gel

bands were cut out and sent for mass spectrometry analysis by the Vincent J. Coates Proteomics/Mass Spectrometry Laboratory at UC Berkeley.

Immunoprecipitation of endogenous protein complexes

To confirm the interaction of endogenous proteins, we lysed Hela cells or D3 mESCs by freeze-thaw twice in 20mM HEPES buffer pH7.5, 5mM KCl, 1.5mM MgCl2, 1x protease inhibitor cocktail (Roche). Specific antibodies against Cul3, Sec13 or Sec31 conjugated to protein G agarose beads were added to the cleared cell lysate and incubated at 4C for 4h. Protein complexes were eluted with gel-loading buffer at 95ºC. Endogenous proteins in complexes were detected by immunoblot using specific antibodies against Cul3, Sec13, Sec31, or Klhl12.

To detect ubiquitination of endogenous COPII components, we incubated Hela cell extract with pre-immune serum or antibody against Sec13 conjugated to protein G agarose beads at 4C for 4h. Protein complexes were eluted with SDS gel-loading buffer at 95ºC. Ubiquitinated proteins in the complex were detected by immunoblot against ubiquitin.

In-vitro protein interaction assays

To dissect the Klhl12 and Sec31A interaction, we coupled 20ug recombinant ^{MBP}Klhl12, various mutants or MBP as a control to 15ul amylose resin by incubating at 4C for 1h. Cul3, Sec31A and mutants were expressed from pCS2 and labeled with ^{35}S-Met using TnT Sp6 Quick Coupled Trsnc/trans Syst (Promega, cat. # L2080). The labeled Cul3 or Sec31A were incubated with MBP-Klhl12 or mutants at 4C for 3h. Beads were washed 4x with TBST and 2x with TBS, and incubated in SDS loading buffer at 95ºC. Samples were run on SDS-PAGE and results were visualized by autoradiography.

In vitro ubiquitination assays with Cul3^{Klhl12}

Cul3/Rbx1 was conjugated to NEDD8 at 30C for 1h with the following conditions: 2.5 mM Tris/HCl pH 7.5, 5 mM NaCl, 1 mM MgCl2, 1 mM DTT, 1x energy mix [40], 1uM APPBP1-UBA3, 1.2 uM Ubc12, 4 uM Cul3/Rbx1, and 60 uM NEDD8. For in-vitro ubiquitination of Sec31A, we set up a 10ul reaction as follows: 2.5 mM Tris/HCl pH 7.5, 5 mM NaCl, 1 mM MgCl2, 1 mM DTT, 1x energy mix, 100nM UBA1, 1uM UbcH5c, 1uM Cul3~Nedd8/Rbx1, 1uM Klhl12, 150uM ubiquitin, 0.05ug Sec13/31A. The reaction was carried out at 30C for 1hr and stopped by adding SDS gel loading buffer.

In vivo ubiquitination assays with Cul3^{Klhl12}

293T cells grown in 10cm dishes were transfected with pCS2-HA-Sec13/31A, pCS2-His-ubiquitin, pcDNA5-Klhl12-FLAG, pcDNA4-Cul3-FLAG, or pcDNA4-Cul3^{N250}-FLAG, as indicated, using calcium phosphate. 24h later, 1μM MG132 was added and cells were incubated overnight. Cells were harvested with gentle scraping and resuspended in 1ml buffer A (6M guanidine chloride, 0.1 M Na_2HPO_4/NaH_2PO_4 and 10mM immidazole,pH 8.0). Cells were lysed by sonication for 10s and incubated with 25ul Ni-NTA agarose at room temperature for 3h. The beads were washed 2x with buffer A, 2x with buffer A/TI (1 volume buffer A and 3 volumes buffer TI), 1x with buffer TI (25mM Tris-Cl, 20mM imidazole, pH6.8), and incubated in 60ul SDS gel loading buffer containing 300mM imidazole and 50mM β ME at 95ºC. Samples were separated by SDS-PAGE and ubiquitinated Sec31A was detected by immunoblot using antibody against Sec31A.

To detect Sec31A ubiquitination upon Cul3/Klhl12 depletion, we co-transfected 100nM siRNAs against Cul3 or Klhl12 with pCS2-HA-Sec13/31A and pCS2-His-ubiquitin using calcium phosphate. The Ni-NTA purification was performed 48h post transfection and Sec31A ubiquitination was detected as described above.

Confocal microscopy

Cells were fixed in 4% paraformaldehyde and permeabilized with 0.5% TritonX-100 in 1X TBS, 2% BSA. Cells were incubated with primary antibodies against Sec31A, Sec13, Sec24C, ERGIC53, CD63, BiP, or ubiquitin for 2h and secondary antibodies (Invitrogen, Alexa Fluor® 546 goat anti-rabbit IgG (H+L); Alexa Fluor 488 goat anti-mouse IgG (H+L); HOECHST 33342,) for 1h at room temperature followed by extensive washing. Pictures were taken on Zeiss LSM 510 and 710 Confocal Microscope systems and analyzed with LSM image browser and Imaris 3D imaging processing software.

Transmission Electron Microscopy

Mock- and Klhl12-transfected HeLa cells were grown to 70% confluence as a monolayer on an Aclar ® sheet (Electron Microscopy Sciences, Hartfield , PA). The cells were fixed for 30min in 0.1M cacodylate buffer, pH 7.2, containing 2% glutaraldehyde, and subsequently washed with buffer prior to post-fixation with 1% Osmium tetroxide on ice. This was followed by staining with 1 % aqueous Uranyl Acetate for 30 min at room temperature. For dehydration with progressive lowering of temperature, each incubation period was 10 min, with exposure to 35% ethanol at 4°C, to 50% ethanol and 70% ethanol at −20°C, and 95%, and 100% ethanol at −35°C. Cells were restored to room temperature in 100% ethanol before flat embedding in an Epon resin. Thin (70-100nm) sections were collected on Formvar-coated 200-mesh copper grids and post-stained with 2% aqueous uranyl acetate and 2% tannic acid. The sections were imaged at 120 kV using a Tecnai 12 Transmission Electron Microscope (FEI, Eindhoven, Netherlands).

For the purpose of immunolabeling, HeLa cells expressing ^{FLAG}Klhl12 or doxycycline-inducible 293T Trex ^{FLAG}Klhl12 stable cell lines were fixed in 2% paraformaldehyde and 0.5% glutaraldehyde and embedded in LR white resin. Fixation

and infiltration were performed in a microwave oven (Pelco model 3450, Ted Pella, Inc., Redding, CA). 70 nm thick sections were picked on 100-mesh nickel grids coated with Formvar film and carbon, incubated in blocking buffer (5% BSA, 0.1% fish gelatin, 0.05% Tween20 in PBS) for 30 min, and followed by incubation with αFLAG antibody at a dilution of 1/40 for 1h. Goat anti-mouse IgG conjugated with 10 nm gold (BD Biosciences) was used as the secondary antibody at a diltuion of 1/40 for 1 h. Sections were poststained in 2% uranyl acetate for 5 min.

Gene expression analysis by microarray

To compare gene expression profiles of WT-mESCs versus Cul3-depleted mESCs, we transfected D3 mESCs with control or Cul3-siRNA, followed by growth on gelatin-coated 6-well plates. 48h later, total RNA was extracted by TRIzol and chloroform, and further purified using RNeasy Mini Kit (Qiagen, cat. # 74104). Microarray analysis was performed by the Functional Genomics Laboratory (UC Berkeley) using Affymetrix Mouse 430A 2.0 chip.

Analysis of collagen export from cells

IMR-90 human lung fibroblasts grown on 100mm dishes in DMEM/10% FBS were transfected with ^{FLAG}Klhl12, ^{FLAG}Klhl12^{FG289AA}, ^{FLAG}Keap1 and pcDNA5-flag using nucleofection kit R (bought from Lonza) as described in the manufacturer's protocol and plated on 6 well plate with 25mm coverslips. When indicated, co-transfections with 2μg each of ^{FLAG}Klhl12 and dominant-negative Cul3 were performed. Dialyzed 10% FBS media was used for ascorbate free transfections. Brefeldin A (Sigma) was used at a concentration of 2.5mg/ml and cells were incubated for 30min. MG132 was used at 20μM for 2h, choloroquine was used at 200μM for 1h. Media was collected the next day

and cells on coverslips were fixed with 3% paraformaldehyde for 30min and remaining cells on a plate were used to prepare lysates. Cells on coverslips were permebealized with 0.1% Triton for 15min at room temperature followed by blocking with 1%BSA for 30min. Primary antibodies used were polyclonal anti Procollagen (LF-67,diluted 1:1000) and anti-flag (diluted 1:200). Secondary antibodies were Alexa fluor 546 donkey anti-rabbit IgG and Alexa Fluor 488 goat ant-rabbit IgG (diluted 1:200). After staining cells with appropriate primary and secondary antibodies, we fixed coverslips on slides using mounting reagent containing DAPI. Images were analyzed with a Zeiss LSM710 confocal microscope and captured with Zen10 software. Merges of images were performed with ImageJ and LSM image Browser. Media collected from 6-well plates was normalized with respect to lysate protein concentration estimated using BCA method. Media and lysates of each reaction were checked by immunoblot analysis. Tubulin was used as loading control for lysates. Ascorbate chase experiments were done by adding ascorbate (0.25mM ascorbic acid and 1mM asc-2-phosphate) to Klhl12-transfected cells, followed by incubation for 5, 10, 30 and 60min.

A human fibrosarcoma cell line (HT1080) stably transfected with proalpha1(1) was used for Cul3 knockdowns. Cul3- and Klh12-shRNAs targeting two different regions in both genes were cloned into pSuperGFP and transfected using Lipofectamine 2000. pSuper GFP was used as negative control. Cells were grown on 25 mm coverslips in 6-well plates and fixed 2d post transfection. Collagen staining was done using LF-67 (1:1000) and ER was stained with anti-PDI (1:1000) antibody. Fibronectin and EGFR were stained in parallel experiments. Fibronectin expression was induced in HT1080 using 1uM dexamethasone before Cul3 knockdowns. ER retention or secretion was scored in cells expressing GFP shRNAs. Cells without GFP shRNAs and transfected with pSUPER GFP were quantified as well. Images were taken on a Zeiss LSM 710

confocal microscope and visualized with LSM image browser. Lysates were prepared from remaining cells on 6 well and checked for knockdown efficiency.

siRNA oligos used in this study

RNAi oligos	Targeted sequence (5' – 3')
mCul3 #1	GAAGGAATGTTTAGGGATA
mCul3 #2	GGAAGAAGATGCAGCACAA
mCul3 #3	GGTGATGATTAGAGACATA
mCul3 #4	CAACTTTCTTCAAACACTA
mCul3 #5	CATTATTTATTGATGATAA
mUBA3	CGTTTGAAGCAGAGAGAAA
mKlhl12	CCTTGAGAGTGGAGCAGAA
hKlhl12	CCAAAGACATAATGACAAA
mKBTBD8	GAACATGAGCAGAGTGAAA
mOct4	AGGCAAGGGAGGTAGACAA
hSec31	CCTGAAGTATTCTGATAAA
mSec13 (pool of 4 oligos)	CCATGTGTTTAGTAATTTA
	GGCAATATGTGGTCACCTA
	GCTGAAAGTATTCATGTAA
	GGAACAAATGACTATTATT
mCdc42 (pool of 4 oligos)	GATCTAATTTGAAATATTA
	GGATTGAGTTCCTAATTAA
	AGAGGATTATGACAGACTA
	AAATCAAACTAAAGATTAA
mBcar1/CAS (pool of 4 oligos)	GACTAATAGTCTACATTTA
	GGAGGTGTCTCGTCCAATA
	CTATGACAATGTTGCTGAA
	GGGCGTCCATGCTCCGGTA
mSrc (pool of 4 oligos)	CCCTTGTGTCCATATTTAA

	CCACGAGGGTTGCCATCAA
	CAGACTTGTTGTACATATT
	GCAACAAGAGCAAGCCCAA
mRhoG (pool of 4 oligos)	GGTTTACCTAAGAGGCCAA
	GCTGTGCCTTAAGGACTAA
	GCACAATGCAGAGCATCAA
	GGCGCACCGTGAACCTAAA
mRhoA (pool of 4 oligos)	GGATTTCCTAATACTGATA
	GAAAGTGTATTTGGAAATA
	AGCCCTATATATCATTCTA
	CGTCTGCCATGATTGGTTA
mRac1 (pool of 4 oligos)	GGTTAATTTCTGTCAAACA
	GCGTTGAGTCCATATTTAA
	GCTTGATCTTAGGGATGAT
	GGAGTAATTCAACTGAATA
mCdh1/E-cadherin (pool of 4 oligos)	GGAGGAGAACGGTGGTCAA
	CGCGGATAACCAGAACAAA
	CCATGTTTGCTGTATTCTA
	GGGACAATGTGTATTACTA
mIqgap1 (pool of 4 oligos)	ACATGATGATGATAAACAA
	GGTTGATTTCACAGAAGAA
	GTATAAATTTATTTCTTAA
	GGTGGATCAGATTCAAGAA
mCul1 (pool of 2 oligos)	GCATGATCTCCAAGTTAAA
	CGTGTAATCTGCTATGAAA
mCul2 (pool of 2 oligos)	GCGCTGATTTGAACAATAA
	CCAGAGTATTTATATCTAA
mCul4a (pool of 2 oligos)	GTGTGATTACCATAATAAA
	CCAGGAAGCTGGTCATCAA

mCul5 (pool of 2 oligos)	CCCTCATATTTACAGCAAA
	ACATGAAGTTTATAATGAA
mCul7 (pool of 2 oligos)	GCATCAAGTCCGTTAATAA
	GGATGTGATTGATATTGAA

Table 1: Identification of BTB proteins that bind Cul3 in mESC extracts
^{FLAG}Cul3 was immobilized on beads and incubated with mESC extracts. Specifically co-purifying proteins were identified on SDS-PAGE and the identity of these proteins was determined by LC/MS.

gene name	# of peptide	# of total peptide	sequence coverage	peptide
BTBD1	1	1	3.30%	K.YAVPALEAHCVEFLTK.H
BTBD2	3	4	3.70%	R.ADNAFMLLTQAR.L R.ADNAFM*LLTQAR.L R.LFNAVVR.W
BTBD9	2	5	4.40%	K.YGAQVVKGELK.S R.APSASSLPPSPGPNSR.S
Enc1	2	3	3.10%	R.M*CLSNFQTIR.K K.AAPM*LVAR.F
Gan	1	2	1.80%	K.NILAAASPYIR.T
Ibtk	11	22	10.60%	R.LGHGDEQTCLVPR.L K.KADILPNLHHSSSDVSCVPDTNSVYER.I R.LEKLPFAHR.A K.TSLYEIPVVSSSSFFEEFGK.L K.SAFEVYRSNQAHTLSER.Q R.SNQAHTLSER.Q R.SNQAHTLSERQK.S R.KRSDSSGGYTLSDVIQSPPSAGLLK.S R.SDSSGGYTLSDVIQSPPSAGLLK.S R.DLQSPDFTAGFHSDKVEGK.A R.TIM*ETEENRQK.Y
Ipp	1	2	1.90%	R.SFEVYDPLSKR.W
Ivns1abp	2	4	3.90%	K.VINWVQR.S R.YNPENNTWTLIAPM*NVAR.R
KBTBD2	9	23	14.10%	R.AWFQGLPPNDK.S K.SVVVQGLYK.S K.SVVVQGLYK.S K.SVVVQGLYKSM*PK.F K.VGTVVTPDNDIYIAGGQVPLK.N K.VGTVVTPDNDIYIAGGQVPLKNTK.T K.TSKLQTAFR.T K.MAANIPAKR.Y K.M*AANIPAKR.Y
KBTBD4	2	5	5.40%	K.HGGDLYVVGGSIPR.R K.TLQDTLSNAVIYYR.V
KBTBD8	7	23	11.50%	R.SM*FTSGLTESTQK.E R.SMFTSGLTESTQKEVR.I R.SM*FTSGLTESTQKEVR.I K.IPPQFAQAIVK.S K.QTVPCLDIVTGR.V R.VYEGDGRNSLK.S R.KNSLYQYDDIADQWM*K.V
KCTD2	2	3	8.40%	R.GHGRQPAAAAQPLEPGPGPPER.A K.ELAEEGVLEEAEFYNIASLVR.L
KCTD3	2	3	5.40%	R.DDQQVFIQK.V R.ESDGGLEVHRTAEGLSEPK.K
KCTD9	4	10	33.80%	R.ADLSGSVLDCANLQGVK.M K.GVDMEGSQM*TGINLR.V

				K.GVDM*EGSQM*TGINLR.V
				K.GAIFEEM*LTPLHM*SQSVR.-
KCTD10	1	1	4.80%	R.M*EVLTDSEGWILIDR.C
Klhdc5	4	9	8.30%	K.SKLIEQSDYFR.A
				K.LIEQSDYFR.A
				R.LVLDFINAGGAR.E
				R.SSQSEDM*LTVQSYNTVTR.Q
Klhl2	13	75	19.20%	R.IKEVDGWTLR.M
				R.EYLVQRVEEEALVK.N
				K.YHLLPTEQR.M
				R.LRTPM*NLPK.L
				R.TPM*NLPK.L
				K.LMVVVGGQAPK.A
				K.LM*VVVGGQAPK.A
				K.LM*VVVGGQAPKAIR.S
				R.TVDSYDPVKDQWTSVANMR.D
				K.SNEWFHVAPM*NTR.R
				R.KSVEVYDPTTNAWR.Q
				K.SVEVYDPTTNAWR.Q
				R.SYAGVTVIDKPL.-
Klhl3	2	6	2.30%	K.AFKVM*NELR.S
				R.LPLLPR.D
Klhl8	2	5	1.70%	R.GGVGIATVMGK.I
				R.GGVGIATVM*GK.I
Klhl9	5	6	10.20%	R.AMMASASDYFK.A
				R.AM*M*ASASDYFK.A
				R.SDSTHLVTLGGVLR.Q
				R.M*NEWSYVAK.M
				R.ACTLTVFPPEENPGSPSRESPLSAPSDHS
Klhl12	5	11	5.90%	K.SILNSM*NSLR.K
				K.SILNSM*NSLRK.S
				R.MPLLTPR.Y
				R.M*PLLTPR.Y
				R.TDSWTTVTSMTTPR.C
Klhl13	6	18	8.20%	R.VM*MASASDYFK.A
				R.VM*M*ASASDYFK.A
				R.M*YDEKTHEWK.S
				K.GKTAVDTVFR.F
				R.TNEWTYVAK.M
				K.VFDLPESLGGIR.A
Klhl18	2	2	2.10%	R.GYGVMEEIR.R
				K.NCLGVR.Q
Klhl20	3	5	5.50%	R.LPLLSPK.F
				K.FLVGTVGSDPLIK.S
				R.TNQWSPVVAM*TSR.R
Klhl22	7	51	11.00%	R.STQHSQALLR.G
				K.NFVAFSR.T
				R.FPLMEAEVLQR.L
				K.YLNPLLGEWK.H
				K.EVYAHAGTTLQGK.M
				R.DVHQVACYSCTSR.Q
				R.SLLHEQPR.G
Klhl24	2	3	3.30%	R.FADTHSLK.T
				R.YHILGNEM*M*SPR.T
Klhl25	3	6	5.90%	R.SSTGSM*NISVFHK.A
				K.ILLNDGVVTSPFAR.P

				K.AAPMLIAR.F
Klhl26	5	11	12.60%	R.SDVASLVAFGGTPYTDSDRAVSSK.V K.VFQLPEPGAR.H R.TWGHAGAAAAGR.L R.LYISGGYGVSAEDKK.A R.VLHAM*LGAAGR.I
Rcbtb1	1	1	2.80%	K.NNLLSPTQIM*VEKER.V
RHOBTB3	2	2	3.90%	R.SPLVSGDESSLLLNAASTVAR.P R.NLIGGADIIVIK.Y
Zbtb11	1	1	5.00%	K.SAVQQVAQK.L

Table S2: Identification of Klhl12-binding proteins
^{FLAG}Klhl12 was immunoprecipitated from 293T cells. Bands were cut out from gels and proteins were identified by LC/MS.

gene name	peptide
BAND1: Sec31A	LIWGPYK
	IIAGDKEVVIAQNDK
	EVVIAQNDK
	QVQHILASASPSGR
	ILASASPSGR
	ATVWDLR
	LPVIQMWDLR
	NPAVLSAASFDGR
	ISVYSIMGGSTDGLR
	SIMGGSTDGLR
	VLPLK
	RPVGASFSFGGK
	LVTFENVR
	KIDASQTEFEK
	IDASQTEFEK
	NVWSFLK
	VNFEDDSR
	YLELLGYR
	VDGANVALK
	DSDQVAQSDGEESPAAEEQLLGEHIK
	LITAVVMK
	AQDGSHPLSLQDLIEK
	AQGEPVAGHE(**pS**)PKIPYEK
	TGPQNGWNDPPALNR
	TTFEDLIQR
	LEFLYDK
	EQTLSPTITSGLHN
	EQTLSPTITSGLHNIAR
	NYSEGLTMH
	IVSTSNFSETSAFMPVLK
	VVLTQANK
BAND2: Sec13	FASGGCDNLIK